

# **MODELING AND ANALYSIS OF A SELF EXCITED INDUCTION GENERATOR DRIVEN BY A WIND TURBINE**

A THESIS SUBMITTED IN PARTIAL FULFILLMENT  
OF THE REQUIREMENTS FOR THE DEGREE OF

**Master of Technology**

In

**Power Control and Drives**

By

**CH SUBHRAMANYAM**

**Roll No. 211EE2141**



**Department of Electrical Engineering  
National Institute of Technology, Rourkela  
Rourkela-769008**

# **MODELING AND ANALYSIS OF A SELF EXCITED INDUCTION GENERATOR DRIVEN BY A WIND TURBINE**

A THESIS SUBMITTED IN PARTIAL FULFILLMENT  
OF THE REQUIREMENTS FOR THE DEGREE OF

**Master of Technology**

In

**Power Control and Drives**

By

**CH SUBHRAMANYAM**

**Roll No. 211EE2141**

**Under The Supervision of**

**Prof. K.B. MOHANTY**



**Department of Electrical Engineering  
National Institute of Technology, Rourkela  
Rourkela-769008**



DEPARTMENT OF ELECTRICAL ENGINEERING  
NATIONAL INSTITUTE OF TECHNOLOGY ROURKELA  
ODISHA, INDIA

## CERTIFICATE

This is to certify that the Thesis entitled **“MODELING AND ANALYSIS OF A SELF EXCITED INDUCTION GENERATOR DRIVEN BY A WIND TURBINE”**, submitted by Mr. CH SUBHRAMANYAM bearing roll no. 211EE2141 in partial fulfillment of the requirements for the award of Master of Technology in Electrical Engineering with specialization in **“Power Control and Drives”** during session 2011-2013 at National Institute of Technology, Rourkela is an authentic work carried out by him under our supervision and guidance.

To the best of our knowledge, the matter embodied in the thesis has not been submitted to any other university/institute for the award of any Degree or Diploma.

Date: 31/12/2013

Place: Rourkela

**Prof. K. B. MOHANTY**  
Dept. of Electrical Engg.  
National Institute of Technology  
Rourkela - 769008

## **ACKNOWLEDGEMENTS**

I would like to express my sincere gratitude to my supervisor **Prof. K. B. MOHANTY** for guidance, encouragement, and support throughout the course of this work. It was an invaluable learning experience for me to be one of their students. From them I have gained not only extensive knowledge, but also a careful research attitude.

I express my gratitude to **Prof. A. K. Panda**, Head of the Department, Electrical Engineering for his invaluable suggestions and constant encouragement all through the thesis work.

My thanks are extended to my colleagues in power control and drives, who built an academic and friendly research environment that made my study at NIT, Rourkela most fruitful and enjoyable.

I would also like to acknowledge the entire teaching and non-teaching staff of Electrical department for establishing a working environment and for constructive discussions.

**CH SUBHRAMANYAM**

**Roll. no.:- 211EE2141**

**M.Tech PCD**

## **ABSTRACT**

Wind energy is one of the most important and promising source of renewable energy all over the world, mainly because it is considered to be non-polluting and economically viable. At the same time there has been a rapid development of related wind energy technology. However in the last two decades, wind power has been seriously considered to supplement the power generation by fossil fuel and nuclear methods. The control and estimation of wind energy conversion system constitute a vast subject and are more complex than those of dc drives. Induction generators are widely preferable in wind farms because of its brushless construction, robustness, low maintenance requirements and self protection against short circuits. However poor voltage regulation and low power factor are its weaknesses.

A large penetration of wind generation into the power system will mean that poor power quality and stability margins cannot be tolerated from wind farms. This paper presents modeling, simulation and transient analysis of three phase self-excited induction generator (SEIG) driven by a wind turbine. Three phase self-excited induction generator is driven by a variable-speed prime mover such as a wind turbine for the clean alternative renewable energy in rural areas. Transients of machine self-excitation under three phase balanced load conditions are simulated using a Matlab/Simulink block diagram for constant, step change in wind speed and random variation in wind speed.

# **CONTENTS**

ABSTRACT	i
CONTENTS	ii
LIST OF FIGURES	v
LIST OF TABLES	vii

## **CHAPTER-1**

### **INTRODUCTION**

1.1 Motivation	2
1.2 Literature Review	2
1.3 Thesis Objectives	3
1.4 Organization of thesis	4

## **CHAPTER-2**

### **WIND ENERGY**

2.1 Source of wind	6
2.2 Wind turbine	7
2.2.1 Vertical axis wind turbine	7
2.2.2 Horizontal axis wind turbine	8
2.3 Power extracted from wind	9
2.4 Torque developed by a wind turbine	11
2.5 tip-speed ratio	12
2.6 power control in wind turbines	13
2.6.1 Pitch control	14
2.6.2 Yaw control	14
2.6.3 Stall control	15
2.7 Summary	15

**CHAPTER-3**  
**AXES TRANSFORMATION**

3.1	Introduction	17
3.2	General change of variables in transformation	17
3.2.1	Transformation into a stationary reference frame	17
3.2.2	Transformation into a rotating reference frame	20
3.3	Summary	21

**CHAPTER-3**  
**THE SEIG SYSTEM**

4.1	Introduction	23
4.2	SEIG system configuration	23
4.3	The Self-Excitation Phenomenon	24
4.3.1	SEIG System Performance	25
4.3.2	Operational Problems of the SEIG System	25
4.4	Summary	26

**CHAPTER-5**  
**MODELLING OF STAND ALONE WIND DRIVEN SEIG SYSTEM**

5.1	Modelling of wind turbine	28
5.2	Modelling of self-excited induction generator	29
5.3	Modelling of excitation capacitor	32
5.4	Modelling of load impedance	33
5.5	Development of wind driven SEIG dynamic model in matlab/simulink	35

5.6 Summary	36
-------------	----

**CHAPTER-6**  
**RESULTS & DISCUSSION**

6.1 Simulation results	38
6.1.1 Self-excitation Process	39
6.1.2 Insertion of Load	41
6.1.3 Loss of Excitation due to heavy-load	41
6.1.4 Insertion of Excitation Capacitor	43
6.1.5 Step change in wind velocity	46
6.2 Experimental results	47

**CHAPTER-7**  
**CONCLUSION & SCOPE OF FUTURE WORK**

7.1 Conclusion	52
7.2 Scope of Future work	52

<b>REFERENCES</b>	<b>53</b>
-------------------	-----------



## LIST OF FIGURES

Fig.2.1 Vertical axis wind turbine í í í í í í í í í í í í í .....07

Fig. 2.2 Horizontal axis wind turbine

(a) Upwind machine (b) downwind machine í í í í í .....08

Fig.2.3. Detail of a wind turbine driven power generation system í í í í ..11

Fig. 2.4 Wind Turbine output torque as a function of turbine Speed í í .....12

Fig. 2.5 Power Coefficient (vs.) Tip Speed Ratio Curve í í í í í í í í .13

Fig 3.1 Three-axes and two-axes in the stationary reference frame í í í ...18

Fig 3.2 Steps of the abc to rotating dq axes transformation

(a) abc to stationary dqaxes (b) stationary  $d^s$ - $q^s$  to rotating  $d^e$ - $q^e$  axes í í .20

Fig. 4.1. Schematic diagram of a standalone SEIG í í í í í í í í í í í ..23

Fig. 5.1 Schematic d-q axes diagram of í í í í í í í í ..í í .....29

Fig. 5.2 d-q model of induction machine in the stationary reference frame í í .30

(a) d-axis (b) q-axis

Fig.5.3 Flow chart for dynamics of Wind Turbine model í í í í í í í í 35

Fig.6.1 SEIG Rotor speed í .40

Fig. 6.2 Magnetizing current í í í í ..í í í í í í í í ..í í .....40

Fig.6.3 Magnetizing Inductance í í í í í í í í í í í í í í í í í í .....40

Fig.6.4 Stator terminal Voltage í í í í í í í í í í ..í í í í í í í í ...40

Fig.6.5 Stator current wave form í í í í í í í í í ..í í í í í í í í í 41

Fig.6.6 SEIG Stator terminal Voltage í í í í í í í í í í í .....42

Fig.6.7 Peak SEIG terminal voltage/phase í í í í í í í í í í í í í ..42

Fig.6.8SEIG rotor speed variation with load	42
Fig. 6.9SEIG stator current waveform	.43
Fig.6.10 Variation of $I_{\mu}$ with load	44
Fig.6.11 Load current variation..	44
Fig.6.12 Loss of excitation..	44
Fig.6.13 Peak SEIG terminal voltage/phase	45
Fig.6.14 Rotor speed variation with load and addition of capacitor.....	45
Fig.6.15 $I_{\mu}$ Variation	45
Fig.6.16 Real power variation	45
Fig.6.17 Reactive power variation	46
Fig.6.18 Step change in wind velocity	46
Fig.6.19 Stator voltage variation with step change	46
Fig.6.20 Rotor speed variation with Step change in wind velocity	47
Fig.6.21 $I_m$ Variation	47
Fig.6.22 Experimental setup	48
Fig.6.23 Build up of Line Voltage	48
Fig.6.24 Settled voltage	49
Fig.6.25 Decrease in voltage by releasing Load	49
Fig.6.26 Reduced voltage after releasing Load	49
Fig.6.27 Increase in voltage by releasing Load	50

## LIST OF TABLES

Table-1 Wind turbine coupled with 22kW induction machine	38
Table-2 Induction machine 22 kW,3-phase,4 Pole star connected, 415 volt,50hz	38
Table-3 Magnetizing inductance vs Magnetizing current	38
Table-4 Wind turbine coupled with 7.5 kW induction machine	38
Table-5 Induction machine 7.5 kW,3-phase,4 pole star-delta connected, 415 volt, 50 Hz	39
Table-6 Magnetizing inductance vs Magnetizing current	38

# CHAPTER 1

## INTRODUCTION

## **1.1MOTIVATION:**

Generation of pollution free power has become the main aim of the researchers in the field of electrical power generation. The depletion of fossil fuels, such as coal and oil, also aid to the importance of switching to renewable and non-polluting energy sources such as solar, tidal and wind energy etc., among which wind energy is the most efficient and wide spread source of energy[1].Wind is a free, clean, and inexhaustible energy source. The high capital costs and the uncertainty of the wind placed wind power at an economic disadvantageous position. In the past four decades methods of harnessing hydro and wind energy for electric power generation and the technology for such alternate systems are developed. From the recent scenario it is also evident that wind energy is drawing a great deal of interest in the power generation sector. If the wind energy could be effectively captured it could solve the problems such as environmental pollution and unavailability of fossil fuel in future. The above fact gives the motivation for development of a wind power generation system which would have better performance and efficiency [2]. Continuous research is going on taking into account different critical issues in this sector.

Induction generators are increasingly being used these days because of their relative advantageous features over conventional synchronous generators. These features are brush-less rugged construction, low cost, less maintenance, simple operation, self protection against faults,good dynamic response and capability to generate power at varying speed. The small-scale power generating system for areas like remotely located single community, a military post or remote industry where extension of grid is not feasible may be termed as stand-alone generating system. Portable gen-sets, stand-by/emergency generators and captive power plants required for critical applications like hospitals, computer centers, and continuous industrial process come under the category of stand-alone generating systems. Self-excited induction generator is best suitable for generating electricity from wind, especially in remote areas, because they do not need an external power supply to produce the excitation magnetic field.

## **1.2LITERATURE REVIEW:**

Several new forms of renewable resources such as wind power generation systems (WPGS) and photovoltaic systems (PV) to supplement fossil fuels have been developed and integrated globally. However, the photovoltaic generation has low energy conversion efficiency and very costly as compared to the wind power, wind generators take a particular place; thus, they

are considered as the most promising in terms of competitiveness in electric energy production. Renewable energy integration in the existing power systems [3] is the demand in future due to the environmental concerns with conventional power plants.

Three phase self-excited induction generator driven by a variable-speed prime mover such as a wind turbine used for the clean alternative renewable energy production. Self-excitation process in induction generators makes the machine for applications in isolated power systems [7]. Various models have been proposed for steady state and transient analysis of self-excited induction generator (SEIG). The d-q reference frame model, impedance based model, admittance based model, operational circuit based model, and power equations based models are frequently used for analysis of SEIG. The overview of self-excited induction generator issues has been provided in this project.

Different constraints such as variation of excitation, wind speed and load have been taken into account and accordingly the effect on generated voltage and current has been analyzed. The effect of excitation capacitance on generated voltage has been analyzed. The dynamic d-q model derived in this paper is based on following assumptions: constant air gap, three phase symmetrical stator and rotor windings, sinusoidal distribution of the air gap magnetic field i.e., space harmonics are neglected. Rotor variables and parameters are referred to the stator windings and core losses are neglected. In this paper, we develop a dynamic model of SEIG, simulate and analyze the transient response of self-excited induction generator. Also transients of machine self-excitation under three phase loading conditions are simulated for constant, step change in wind speed using a Matlab/Simulink block diagram. Also an experiment is conducted in lab on open loop control of SEIG.

### **1.3 THESIS OBJECTIVES:**

The following objectives have been achieved at the end of the project.

- 1) To study about wind as a power source and the mechanism of conversion of wind power to mechanical power and also the variation of output power and output torque with rotor angular speed and wind speed.
- 2) To study the three-axes to two-axes transformation applicable for any balanced three-phase system.
- 3) Study the self-excited induction generator under different load conditions.

- 4) To study the d-q model of self-excited induction generator driven by variable speed prime movers and in particular by wind turbines in stationary reference frame and developing a mathematical model.
- 5) To analyze the effect of speed and excitation capacitance on power variations and line voltages.
- 6) Analyze the dynamic voltages, currents, electromagnetic torque developed by the induction generator and generated output power for a constant, step change and random variation in wind speed.
- 7) Experimentally verify the open loop control on self excited induction generator in the laboratory.

## **1.4 ORGANIZATION OF THESIS:**

The thesis is organized into seven chapters including the introduction in the Chapter 1. Each of these is summarized below.

**Chapter 2:** Deals with the various sources of wind energy and types of wind turbines available. A brief idea is given about how torque and power produced from wind turbines and it is followed by different methods of power control.

**Chapter 3:** Describes the method to convert variables from three axes to two axes and variables transformation into stationary reference frame and also rotating reference frame.

**Chapter 4:** Describes about the stand-alone Self-excited induction generator system. This chapter initially gives an idea of self-excitation phenomena in SEIG and followed by system performance and its operational problems.

**Chapter 5:** Describes the mathematical modelling of wind turbine, self-excited induction generator, excitation capacitor and load impedance.

**Chapter 6:** The simulation results of SEIG at no-load and with RL load at different conditions are showed. Also experimental results of SEIG with open loop control are included in this chapter.

**Chapter 7:** Reveals the general conclusions of the work done and the references.

# CHAPTER 2

## WIND ENERGY



## 2.1 WIND SOURCES

Wind is a result of the movement of atmospheric air. Wind comes from the fact that the regions around the equator, at  $0^\circ$  latitude, are heated more by the sun than the polar region. The hot air from the tropical regions rises and moves in the upper atmosphere toward the poles, while cool surface winds from the poles replace the warmer tropical air. These winds are also affected by the earth's rotation about its own axis and the sun. The moving colder air from the poles tends to twist toward the west because of its own inertia and the warm air from the equator tends to shift toward the east because of this inertia. The result is a large counterclockwise circulation of air streams about low-pressure regions in the northern hemisphere and clockwise circulation in the southern hemisphere. The seasonal changes in strength and direction of these winds result from the inclination of the earth's axis of rotation at an angle of  $23.5^\circ$  to the axis of rotation about the sun, causing variations of heat radiating to different areas of the planet [4].

Local winds are also created by the variation in temperature between the sea and land. During the daytime, the sun heats landmasses more quickly than the sea. The warmed air rises and creates a low pressure at ground level, which attracts the cool air from the sea. This is called a sea breeze. At night the wind blows in the opposite direction, since water cools at a lower rate than land. The land breeze at night generally has lower wind speeds, because the temperature difference between land and sea is smaller at night. Similar breezes are generated in valleys and on mountains as warmer air rises along the heated slopes. At night the cooler air descends into the valleys. Although global winds, due to temperature variation between the poles and the equator, are important in determining the main winds in a given area, local winds have also influence on the larger scale wind system.

Meteorologists estimate that about 1% of the incoming solar radiation is converted to wind energy. Since the solar energy received by the earth in just ten days has energy content equal to the world's entire fossil fuel reserves (coal, oil and gas), this means that the wind resource is extremely large. As of 1990 estimation, one percent of the daily wind energy input, i.e. 0.01% of the incoming solar energy, is equivalent to the world daily energy consumption [5]. It is encouraging to know that the global wind resource is so large and that it can be used to generate more electrical energy than what is currently being used.

## 2.2 WIND TURBINE

A wind turbine is a turbine driven by wind. Modern wind turbines are technological advances of the traditional windmills which were used for centuries in the history of mankind in applications like water pumps, crushing seeds to extract oil, grinding grains, etc. In contrast to the windmills of the past, modern wind turbines used for generating electricity have relatively fast running rotors.

In principle there are two different types of wind turbines: those which depend mainly on aerodynamic lift and those which use mainly aerodynamic drag. High speed wind turbines rely on lift forces to move the blades, and the linear speed of the blades is usually several times faster than the wind speed. However with wind turbines which use aerodynamic drag the linear speed cannot exceed the wind speed as a result they are low speed wind turbines. In general wind turbines are divided by structure into horizontal axis and vertical axis.

### 2.2.1 Vertical axis wind turbine

The axis of rotation for this type of turbine is vertical. It is the oldest reported wind turbine. It is normally built with two or three blades. A typical vertical axis wind turbine is shown in Fig. 2.1. Note that the C-shaped rotor blade is formally called a 'troposkien'.

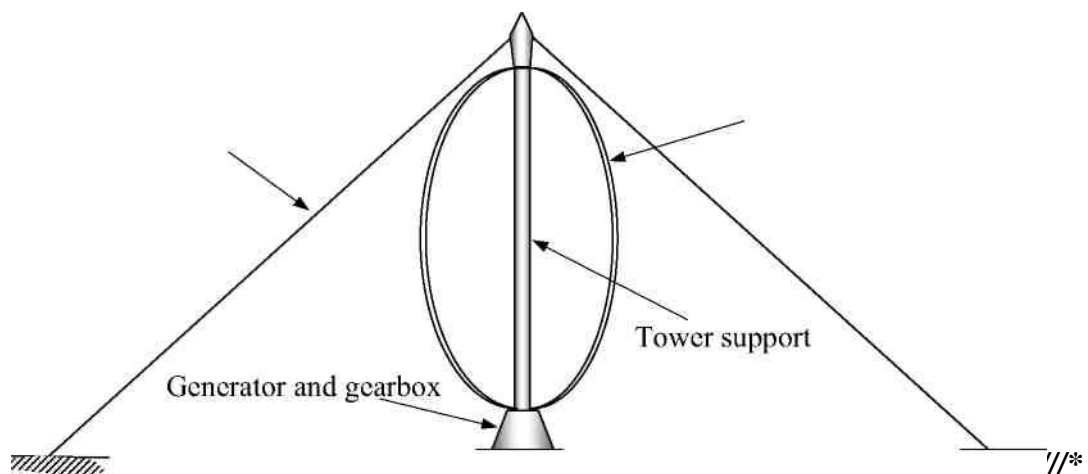


Fig. 2.1 Vertical axis wind turbine

The primary aerodynamic advantage of the vertical axis Darrieus machine is that the turbine can receive the wind from any direction without the need of a yaw mechanism to continuously orient the blades toward the wind direction. The other advantage is that its vertical drive shaft simplifies the installation of gearbox and electrical generator on the ground, making the structure much simpler. On the disadvantage side, it normally requires guy wires attached to the top for support. This could limit its applications, particularly for offshore sites. Wind speeds are very low close to ground level, so although it might save the need for a tower, the wind speed will be very low on the lower part of the rotor. Overall, the vertical axis machine has not been widely used because its output power cannot be easily controlled in high winds simply by changing the pitch. Also Darrieus wind turbines are not self-starting; however straight-bladed vertical axis wind turbines with variable-pitch blades are able to overcome this problem.

## 2.2.2 Horizontal axis wind turbine

Horizontal axis wind turbines are those machines in which the axis of rotation is parallel to the direction of the wind. At present most wind turbines are of the horizontal axis type. Depending on the position of the blades wind turbines are classified into upwind machines and downwind machines as shown in Fig. 2.2. Most of the horizontal axis wind turbines are of the upwind machine type. In this study only the upwind machine design is considered.

Wind turbines for electric generation application are in general of three blades, two blades or a single blade. The single blade wind turbine consists of one blade and a counterweight. The three blades wind turbine has 5% more energy capture than the two blades and in turn the two blades has 10% more energy capture than the single blade. These figures are valid for a given set of turbine parameters and might not be universally applicable.

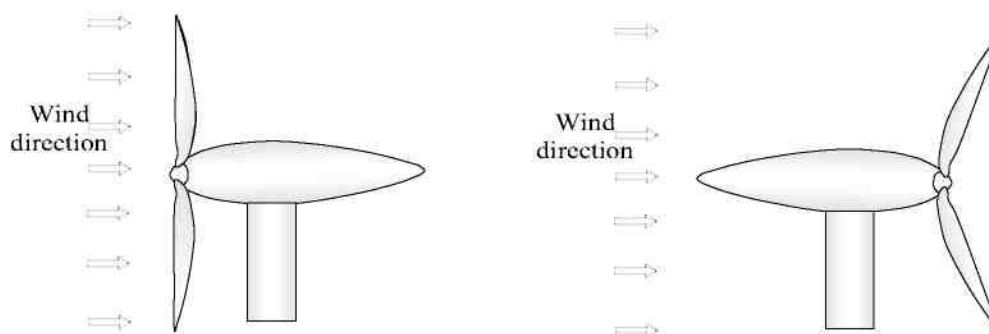


Fig. 2.2 Horizontal axis wind turbine (a) upwind machine (b) downwind machine

The three blade wind turbine has greater dynamic stability in free yaw than two blades, minimizing the vibrations associated with normal operation, resulting in longer life of all components.

## 2.3 POWER EXTRACTED FROM WIND

Air has a mass. As wind is the movement of air, wind has a kinetic energy. To convert this kinetic energy of the wind to electrical energy, in a wind energy conversion system, the wind turbine captures the kinetic energy of the wind and drives the rotor of an electrical generator.

The kinetic energy (KE) in wind is given by

$$KE = \frac{1}{2}mV^2 \quad (2.1)$$

Where  $m$ - is the mass of air in Kg,  $V$ -is the speed of air in m/s.

The power in wind is calculated as the flux of kinetic energy per unit area in a given time, and can be written as

$$P = \frac{d(KE)}{dt} = \frac{1}{2} \frac{dm}{dt} V^2 = \frac{1}{2} \dot{m} V^2 \quad (2.2)$$

where  $\dot{m}$  is the mass flow rate of air per second, in kg/s, and it can be expressed in terms of the density of air ( $\rho$  in kg/m<sup>3</sup>) and air volume flow rate per second ( $\dot{Q}$  in m<sup>3</sup>/s) as given below

$$\dot{m} = \rho \dot{Q} = \rho AV \quad (2.3)$$

Where  $A$ -is the area swept by the blades of the wind turbine, in m<sup>2</sup>.

Substituting equation (2.3) in (2.2), we get

$$P = \frac{1}{2} \rho AV^3 \quad (2.4)$$

Then the ratio of wind power extracted by the wind turbine to the total wind power is the dimensionless power coefficient  $C_p$ , which will also affect the power extracted from wind. So the equation can be written as

$$P = \frac{1}{2} \rho A V^3 C_p \quad (2.5)$$

$$P = \frac{1}{2} \rho \pi D^2 V^3 C_p \quad (2.6)$$

Where  $D$  is the sweep diameter of the wind turbine.

This is the total wind power entering the wind turbine. This calculation of power developed from a wind turbine is an idealized one-dimensional analysis where the flow velocity is assumed to be uniform across the rotor blades, the air is incompressible and there is no turbulence where flow is inviscid (having zero viscosity).

The volume of air entering the wind turbine should be equal to the volume of air leaving the wind turbine because there is no storage of air in the wind turbine. As a result volume flow rate per second,  $Q$ , remains constant, which means the product of  $A$  and  $V$  remains constant. Hence when the wind leaves the wind turbine, its speed decreases and expands to cover more area. The coefficient of power of a wind turbine is a measurement of how efficiently the wind turbine converts the energy in the wind into electricity. The coefficient of power at a given wind speed can be obtained by dividing the electricity produced by the total energy available in the wind at that speed. The maximum value of power coefficient  $C_p$  gives the maximum power absorbed by the wind turbine. In practical designs, the maximum achievable  $C_p$  is below 0.5 for high speed, two blade wind turbines, and between 0.2 and 0.4 for slow speed turbines with more blades.

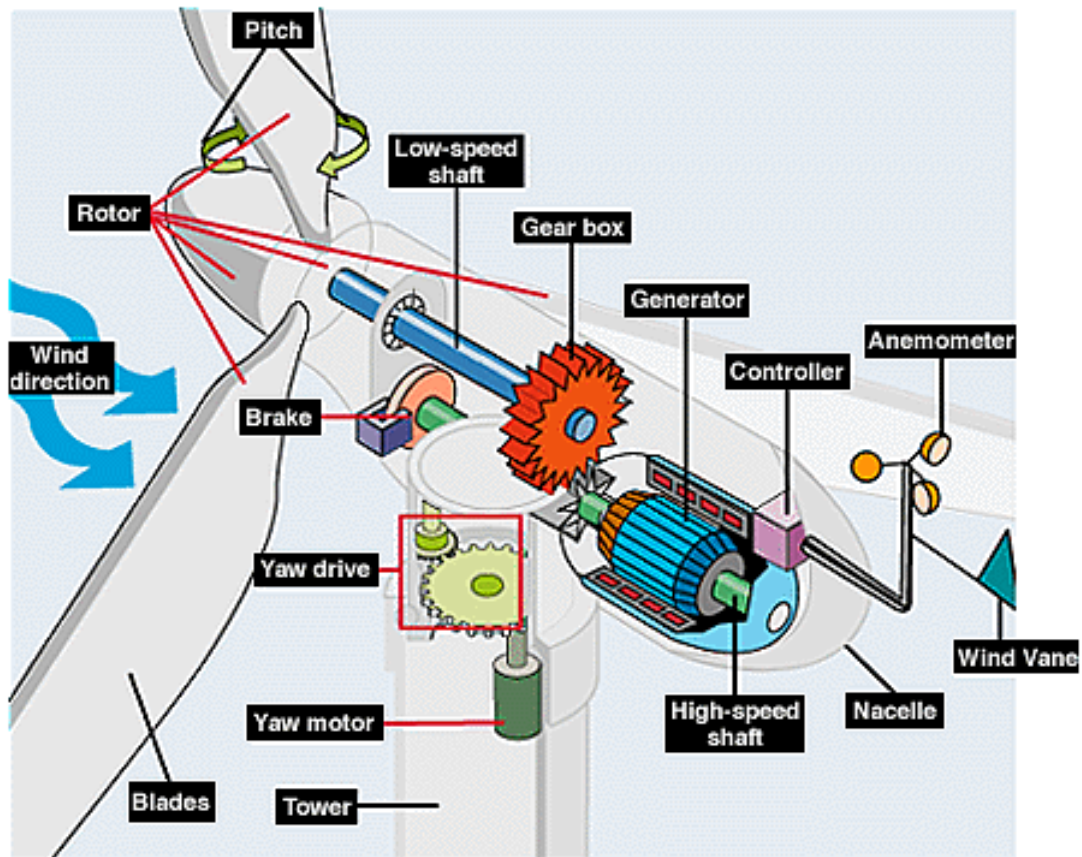


Fig. 2.3 Detail of a wind turbine driven power generation system

## 2.4 TORQUE DEVELOPED BY A WIND TURBINE

The torque in a wind turbine is produced due to the force created as a result of pressure difference on the two sides of each blade of the wind turbine. From fluid mechanics it is known that the pressure in fast moving air is less than in stationary or slow moving air. This principle helps to produce force in an aero plane or in a wind turbine.

On a wind turbine rotor the blades are at some angle to the plane of rotation. At low shaft speeds, the angle of incidence on a blade element at some radius from the hub is large, the blades are stalled and only a small amount of driving force will be created. As a result small torque will be produced at low shaft speed. As the shaft speed increases the velocity

of the wind hitting the blade element increases, because of the additional component of wind due to the blade's rotational speed. In addition, the angle of incidence decreases. If this angle is below the blades stall angle, lift increases and drag decreases, resulting in higher torque. As the shaft speed increases further, the angle of incidence on the blade element decreases towards zero as the free wind speed becomes insignificant relative to the blade's own velocity. Since lift generated by a blade is proportional to the angle of incidence below stall, the torque reduces towards zero at very high shaft speeds. For a horizontal axis wind turbine, operating at fixed pitch angle, the torque developed by the wind turbine,  $T$ , can be expressed as

$$T = \frac{P}{\omega} \quad (2.7)$$

Where  $\omega$  - angular velocity of the wind turbine, rad/s.

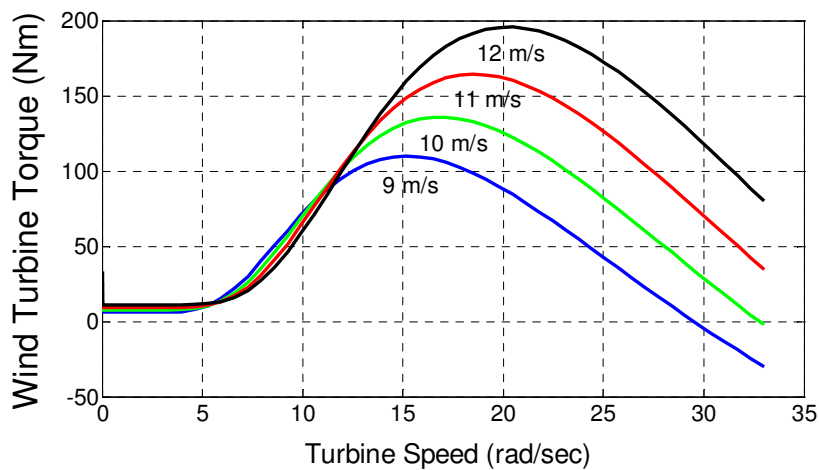


Fig. 2.4 Wind Turbine output torque as a function of turbine Speed

## 2.5 TIP-SPEED RATIO

A tip speed ratio  $TSR$  is simply the rate at which the ends of the blades of the wind turbine turn (tangential speed) in comparison to how fast the wind is blowing. The tip speed ratio  $TSR$  is expressed as:

$$TSR = \frac{V_m}{V_\omega} = \frac{\omega_T r}{V_\omega} \quad (2.8)$$

Where  $V_m$  - tangential speed of the blades at the tips  $\omega_T$ - angular velocity of the wind turbine  $r$  - radius of the wind turbine  $V_w$  - undisturbed wind speed in the site.

The tip speed ratio dictates the operating condition of a turbine as it takes into account the wind created by the rotation of the rotor blades. A typical power coefficient  $C_p$  versus tip speed ratio  $TSR$  is given in Fig. 2.5. The tip speed ratio shows tangential speed at which the rotor blade is rotating compared with the undisturbed wind speed.

As the wind speed changes, the tip speed ratio and the power coefficient will vary. The power coefficient characteristic has single maximum at a specific value of tip speed ratio. Therefore if the wind turbine is operating at constant speed then the power coefficient will be maximum only at one wind speed.

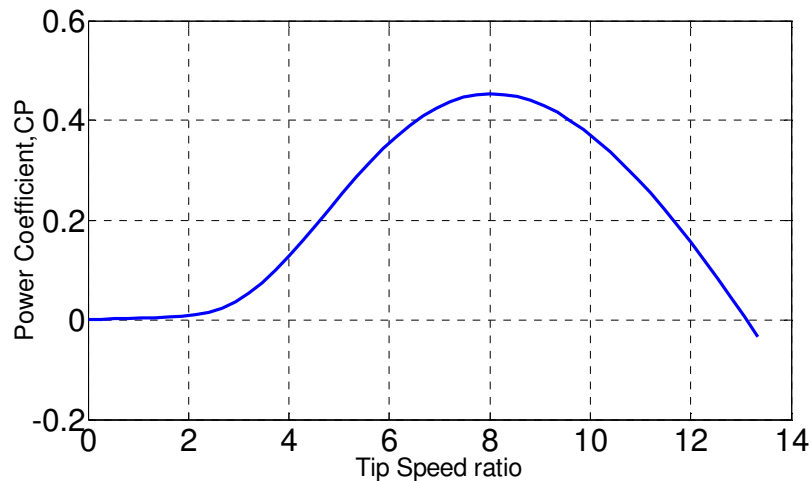


Fig.2.5.Power Coefficient (vs.) Tip Speed Ratio Curve

Usually, wind turbines are designed to start running at wind speeds somewhere around 4 to 5 m/s. This is called the cut in wind speed. The wind turbine will be programmed to stop at high wind speeds of 25 m/s, in order to avoid damaging the turbine. The stop wind speed is called the cut out wind speed.

## 2.6 POWER CONTROL IN WIND TURBINES

The output power of a wind turbine is a function of the wind speed. The determination of the range of wind speed at which the wind turbine is required to operate depends on the probability of wind speed obtained from wind statistics for the site where the wind turbine is



to be located. This histogram is derived from long term wind data covering several years. The histogram indicates the probability, or the fraction of time, where the wind speed is within the interval given by the width of the columns.

In a wind power system typically the wind turbine starts operating (cut in speed) when the wind speed exceeds 4-5m/s, and is shut off at speeds exceeding 25 to 30m/s. In between, it can operate in the optimum constant  $C_p$  region, the speed-limited region or the power limited region . This design choice was made in order to limit the strength and therefore the weight and cost of the components of the wind turbine. Over the year some energy will be lost because of this operating decision

As discussed in Section 2.3 the power absorbed by the wind turbine is proportional to the cube of the wind speed. Hence there should be a way of limiting the peak absorbed power. Wind turbines are therefore generally designed so that they yield maximum output at wind speeds around 15 meters per second. In case of stronger winds it is necessary to waste part of the excess energy of the wind in order to avoid damaging the wind turbine. All wind turbines are therefore designed with some sort of power control to protect the machine. There are different ways of doing this safely on modern wind turbines.

### **2.6.1 Pitch control**

In pitch controlled wind turbines the power sensor senses the output power of the turbine. When the output power goes above the maximum rating of the machine, the output power sensor sends a signal to the blade pitch mechanism which immediately pitches (turns) the rotor blades slightly out of the wind. Conversely, the blades are turned back into the wind whenever the wind speed drops again. On a pitch controlled wind turbine, in order to keep the rotor blades at the optimum angle and maximize output for all wind speeds, the pitch controller will generally pitch the blades by a small angle every time the wind changes. The pitch mechanism is usually operated using hydraulics.

### **2.6.2 Yaw control**

Yaw control is a mechanism of yawing or tilting the plane of rotation out of the wind direction when the wind speed exceeds the design limit. In this way the effective flow cross section of the rotor is reduced and the flow incident on each blade considerably modified.

### **2.6.3 Stall control**

Under normal operating conditions, a stalled rotor blade is unacceptable. This is because the power absorbed by the wind turbine will decrease, even to the point where no power is absorbed. However, during high wind speeds, the stall condition can be used to protect the wind turbine. The stall characteristic can be designed in to the rotor blades so that when a certain wind speed is exceeded, the power absorbed will fall to zero, hence protecting the equipment from exceeding its mechanical and electrical ratings. In stall controlled wind turbines the angle of the rotor blades is fixed. The cross sectional area of the rotor blade has been aerodynamically designed to ensure that the moment the wind speed becomes too high, it creates turbulence on the side of the rotor blade which is not facing the wind. The stall prevents the creation of a tangential force which pulls the rotor blade to rotate. The rotor blade has been designed with a slight twist along its length, from its base to the tip, which helps to ensure that the wind turbine stalls gradually, rather than abruptly, when the wind speed reaches its critical value.

The main advantage of stall control is that it avoids moving parts in the rotor blade itself, and a complex control system. However, stall control represents a very complex aerodynamic design problem, and related design challenges in the structural dynamics of the whole wind turbine, e.g. to avoid stall-induced vibrations. Around two thirds of the wind turbines currently being installed in the world are stall controlled machines.

## **2.7 Summary**

The general definition of wind and the source of wind have been presented in this chapter. The analysis of power absorbed by a wind turbine is based on the horizontal axis wind turbine. The mechanism of production of force from wind that causes the rotor blades to rotate in a plane perpendicular to the general wind direction at the site has been discussed in detail. The importance of having twisted rotor blades along the length from the base to the tip is given. The variation of the torque produced by the wind turbine with respect to the rotor angular speed has been presented.

Power absorbed by a wind turbine is proportional to the cube of the wind speed. Wind turbines are designed to yield maximum output power at a given wind speed. Different ways of power control to protect the machine have been presented.

# CHAPTER 3

## AXES

## TRANSFORMATION

### **3.1 INTRODUCTION**

Mathematical transformations are tools which make complex systems simple to analyze and solutions easy to find. In electrical machines analysis a three-phase axes to two-phase axes transformation is applied to produce simpler expressions that provide more insight into the interaction of the different parameters. The different transformations studied in the past are given in [1]

### **3.2 GENERAL CHANGE OF VARIABLES IN TRANSFORMATION**

A symmetrical three phase machine is considered with three axes at 120 degree apart as shown in fig.2. The three axes are representing the real three phase supply system. However, the two axes are fictitious axes representing two fictitious phases perpendicular, displaced by  $90^\circ$ , to each other. The transformation of three-axes to two-axes can be done in such a way that the two-axes are in a stationary reference frame, or in rotating reference frame. The transformation actually achieves a change of variable, creating the new reference frame. Transformation into a rotating reference frame is more general and can include the transformation to a stationary reference frame. If speed of the rotation of the reference frame is zero it becomes a stationary reference frame.

If the reference frame is rotating at the same angular speed as the excitation frequency, when the variables are transformed into this rotating reference frame, they will appear as a constant value instead of time-varying values.

#### **3.2.1 Transformation into a stationary reference frame**

Here the assumption taken is that the three-axes and the two-axes are in a stationary reference frame. It can be rephrased as a transformation between abc and stationary dq0 axes.

To visualize the transformation from three-axes to two-axes, the trigonometric relationship between three-axes and two-axes is given below.

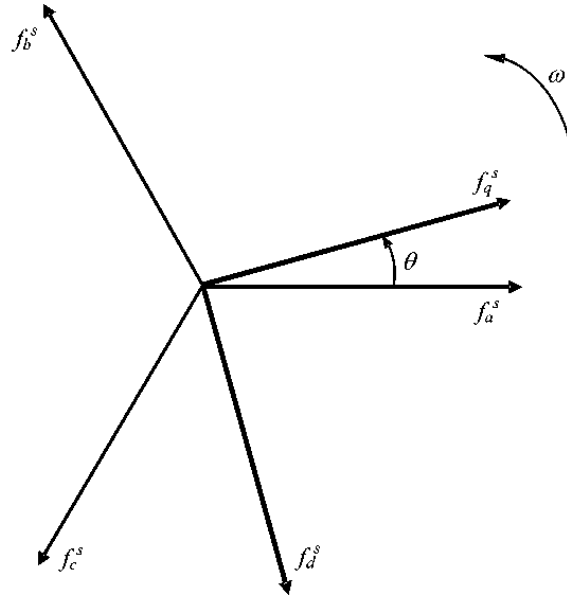


Fig. 3.1 Three-axes and two-axes in the stationary reference frame

In the above diagram, Fig. 3.1,  $f$  can represent voltage, current, flux linkage, or electric charge. The subscript  $s$  indicates the variables, parameters, and transformation associated with stationary circuits. The angular displacement  $\theta$  shows the displacement of the two-axes, dq-axes, from the three-axes, abc-axes.  $f_{qs}$  and  $f_{ds}$  variables are directed along paths orthogonal to each other.  $f_{as}$ ,  $f_{bs}$ , and  $f_{cs}$  may be considered as variables directed along stationary paths each displaced by 120 electrical degrees.

A change of variables which formulates a  $\alpha$ -phase transformation of the three variables of stationary circuit elements to an arbitrary reference frame can be expressed as [1]:

$$\begin{bmatrix} f_q^s \\ f_d^s \\ f_0^s \end{bmatrix} = \frac{2}{3} \begin{bmatrix} \cos \theta & \cos\left(\theta - \frac{2\pi}{3}\right) & \cos\left(\theta + \frac{2\pi}{3}\right) \\ \sin \theta & \sin\left(\theta - \frac{2\pi}{3}\right) & \sin\left(\theta + \frac{2\pi}{3}\right) \\ \frac{1}{2} & \frac{1}{2} & \frac{1}{2} \end{bmatrix} \begin{bmatrix} f_a^s \\ f_b^s \\ f_c^s \end{bmatrix} \quad (3.1)$$

It is important to note that the zero-sequence variables are not associated with the arbitrary reference frame. Instead, the zero-sequence variables are related arithmetically to the abc variables, independent of  $\theta$ .

The inverse of Equation (3.1), which can be derived directly from the relationship given in Fig. 3.1, is

$$\begin{bmatrix} f_a^s \\ f_b^s \\ f_c^s \end{bmatrix} = \begin{bmatrix} \cos \theta & \sin \theta & 1 \\ \cos \left( \theta - \frac{2\pi}{3} \right) & \sin \left( \theta - \frac{2\pi}{3} \right) & 1 \\ \cos \left( \theta + \frac{2\pi}{3} \right) & \sin \left( \theta + \frac{2\pi}{3} \right) & 1 \end{bmatrix} \begin{bmatrix} f_q^s \\ f_d^s \\ f_0^s \end{bmatrix} \quad (3.2)$$

In Fig. 3.1, if the q-axis is aligned with the a-axis, i.e.  $\theta = 0$ , Equation (3.1) will be written as:

$$\begin{bmatrix} f_q^s \\ f_d^s \\ f_0^s \end{bmatrix} = \frac{2}{3} \begin{bmatrix} 1 & -\frac{1}{2} & -\frac{1}{2} \\ 0 & -\frac{\sqrt{3}}{2} & \frac{\sqrt{3}}{2} \\ \frac{1}{2} & \frac{1}{2} & \frac{1}{2} \end{bmatrix} \begin{bmatrix} f_a^s \\ f_b^s \\ f_c^s \end{bmatrix} \quad (3.3)$$

and Equation (3.2) will be simplified to:

$$\begin{bmatrix} f_a^s \\ f_b^s \\ f_c^s \end{bmatrix} = \begin{bmatrix} 1 & 0 & 1 \\ -\frac{1}{2} & -\frac{\sqrt{3}}{2} & 1 \\ -\frac{1}{2} & \frac{\sqrt{3}}{2} & 1 \end{bmatrix} \begin{bmatrix} f_q^s \\ f_d^s \\ f_0^s \end{bmatrix} \quad (3.4)$$

In Equation (3.3) and (3.4) the magnitude of the phase quantities, voltages and currents, in the three (abc) axes and two (dq) axes remain the same. This transformation is based on the assumption that the number of turns of the windings in each phase of the three axes and the two axes are the same. Here the advantage is the peak values of phase voltages and phase currents before and after transformation remain the same.

### 3.2.2 Transformation into a rotating reference frame

The rotating reference frame can have any speed of rotation depending on the choice of the user. Selecting the excitation frequency as the speed of the rotating reference frame gives the advantage that the transformed variables, which had instantaneous values, appear as constant (DC) values. In other words, an observer moving along at that same speed will see the space vector as a constant spatial distribution, unlike the time-varying values in the stationary abc axes.

This reference frame moves at the same speed as the observer. Since we are dealing with two-dimensional variables, the rotating reference can be any two independent basic space vectors, which for convenience another pair of orthogonal dq axes will be used. The zero-sequence component remains the same as before. Fig. 3.3 shows the abc to rotating dq transformation in two steps, i.e., first transforming to stationary dq axes and then to rotating dq axes.

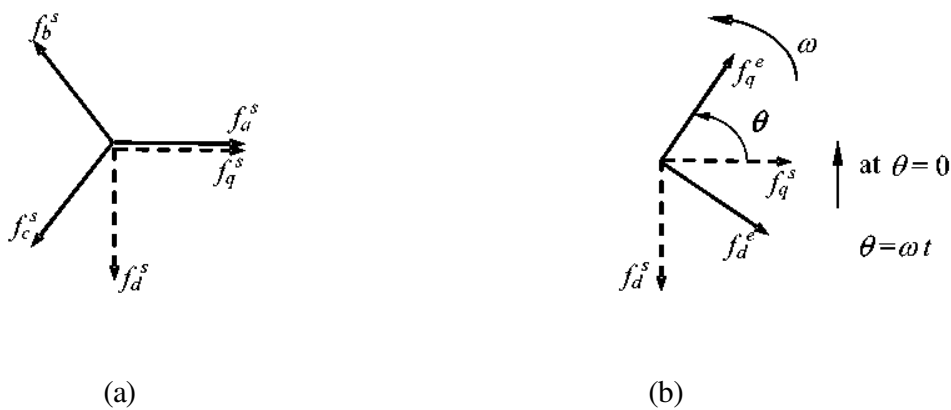


Fig. 3.2 Steps of the abc to rotating dq axes transformation (a) abc to stationary dq axes

b) stationary  $d^s$ - $q^s$  to rotating  $d^e$ - $q^e$  axes

The equation for the abc to stationary dq-axes transformation is given in Equation (3.5). Using geometry, it can be shown that the relation between the stationary  $d^s$ - $q^s$  axes and rotating  $d^e$ - $q^e$  axes is expressed as:

$$\begin{bmatrix} f_q^e \\ f_d^e \end{bmatrix} = \begin{bmatrix} \cos \theta & -\sin \theta \\ \sin \theta & \cos \theta \end{bmatrix} \begin{bmatrix} f_q^s \\ f_d^s \end{bmatrix} \quad (3.5)$$

The angle,  $\theta$ , is the angle between the q-axis of the rotating and stationary d<sup>s</sup>-q<sup>s</sup> axes.  $\theta$  is a function of the angular speed,  $w(t)$ , of the rotating d<sup>e</sup>-q<sup>e</sup> axes and the initial value, that is

$$\theta(t) = \int_0^t w(t) dt + \theta(0) \quad (3.6)$$

If the angular speed of the rotating reference frame is the same as the excitation frequency then the transformed variables in the rotating reference frame will appear constant (DC).

The three phase voltages and currents are obtained by applying d-q to a-b-c transformation equations as above explained

$$\begin{bmatrix} f_a \\ f_b \\ f_c \end{bmatrix} = \begin{bmatrix} 1 & 0 \\ -\frac{1}{2} & -\frac{\sqrt{3}}{2} \\ -\frac{1}{2} & +\frac{\sqrt{3}}{2} \end{bmatrix} \begin{bmatrix} f_{sq} \\ f_{sd} \end{bmatrix} \quad (3.7)$$

where  $f_a$ ,  $f_b$  and  $f_c$  are three phase voltage or current quantities and  $f_{sq}$  and  $f_{sd}$  are the two-phase voltage or current quantities.

### 3.3SUMMARY

The three-axes to two-axes transformation presented in this chapter is applicable for any balanced three-phase system. It has been discussed that the three-axes to two-axes transformation simplifies the calculation of rms current, rms voltage, active power and power factor in a three-phase system. Only one set of measurements taken at a single instant of time is required when using the method described to obtain rms current, rms voltage, active power and power factor. And from measurements taken at two consecutive instants in time the frequency of the three-phase AC power supply can be evaluated.



# CHAPTER 4

## THE SEIG SYSTEM

## 4.1 INTRODUCTION:

As discussed in the previous chapter, renewable energy is the key to our low carbon energy future. The use of an induction machine as a generator is becoming more and more popular for renewable energy applications [8], [9]. Squirrel cage induction generators with excitation capacitors (known as SEIGs) are popular in isolated nonconventional energy systems [17], [22]. The main limitation of the SEIG system is the poor voltage and frequency regulation when supplying variable loads connected to the stator terminals. However, the development of static power converters has facilitated the control of the output voltage and frequency of the induction generator. This chapter presents a literature review of the development, the self-excitation phenomena, the performance and the operational problems of the SEIG system.

## 4.2 SEIG SYSTEM CONFIGURATION

The SEIG system is composed of four main items: the prime mover, the induction machine, the load and the self-excitation capacitor bank. The general layout of the SEIG system is shown in Figure 4.1.

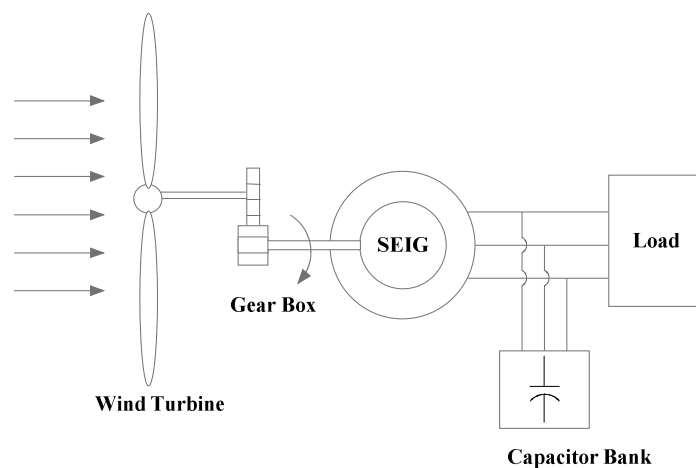


Figure 4.1 Schematic diagram of a standalone self-excited induction generator.

The real power required by the load is supplied by the induction generator by extracting power from the prime mover (turbine). When the speed of the turbine is not regulated, both the speed and shaft torque vary with variations in the power demanded by the loads. The self-excitation capacitors connected at the stator terminals of the induction machine must produce sufficient reactive power to supply the needs of the load and the induction generator.

A squirrel cage induction generator (SCIG) is more attractive than a conventional synchronous generator in this type of application because of its low unit cost, absence of DC excitation source, brushless cage rotor construction and lower maintenance requirement [10]. A suitably sized three-phase capacitor bank connected at the generator terminals is used as variable lagging VAR source to meet the excitation demand of the cage machine and the load. The machine operated in this mode is known as a *Self-excited Induction Generator* (SEIG). However, the main drawback of the standalone SEIG is its poor voltage and frequency regulations under variable loads. A change in the load impedance directly affects the excitation of the machine because the reactive power of the excitation capacitors is shared by both the machine and the load. Therefore, the generating voltage drops when the impedance of the load is increased resulting in poor voltage regulation. Poor frequency regulation occurs (an increase in the slip of the induction machine) when the load is increased.

### **4.3 THE SELF-EXCITATION PHENOMENON**

The self-excitation phenomenon of an induction machine is still under considerable attention although it is known for more than a half century [9],[11]. When a standalone induction machine is driven by a mechanical prime mover, the residual magnetism in the rotor of the machine induces an EMF in the stator windings at a frequency proportional to the rotor speed. This EMF is applied to the capacitors connected to the stator terminals and causes reactive current to flow in the stator windings. Hence a magnetizing flux in the machine is established. The final value of the stator voltage is limited by the magnetic saturation within the machine. The induction machine is then capable of operating as a generator in isolated locations without a grid supply.

Once the machine is self-excited and loaded, the magnitude of the steady-state voltage generated by the SEIG is determined by the nonlinearity of the magnetizing curves, the value of the self-excitation capacitance, speed, machine parameters and terminal loads. As the load and speed of the SEIG changes, the demand for lagging VARs to maintain a constant AC voltage across the machine terminals also changes.

### **4.3.1 SEIG SYSTEM PERFORMANCE**

The performance characteristics of the SEIG system depend mainly on the following:

- a. The parameters of the induction machine
- b. The machine operating voltage, rated power, power factor, rotor speed and operating temperature and the induction machine parameters directly affect the performance of the SEIG system.
- c. The Self-excitation process
- d. The connection of a capacitor bank across the induction machine stator terminals is necessary in the case of standalone operation of the system. The capacitor connection scheme (delta or star) and the use of fixed or controlled self-excitation capacitors have a direct impact on the performance of a SEIG system.
- e. Load parameters
- f. The power factor, starting/maximum torque and current, generated harmonics and load type also affect the performance of the SEIG system directly.
- g. Type of prime mover

Whether the primary source is hydro, wind biomass or combinations, the performance of the SEIG system is affected.

### **4.3.2 OPERATIONAL PROBLEMS OF THE SEIG SYSTEM**

The main operational problem of the SEIG system is its poor voltage and frequency regulation under varying load conditions [11]. A change in the load impedance directly affects the machine

excitation. This is because the reactive power of the excitation capacitors is shared by both the induction machine and the load impedance. Therefore, the generator's voltage drops when the load impedance is increased resulting in poor voltage regulation. On the other hand, the slip of the induction generator increases with increasing load, resulting in a load dependent frequency, even if the speed of the prime mover remains constant.

#### **4.4 SUMMARY**

An overview of the self-excitation phenomenon was presented in this chapter. The performance characteristics and operational problems of SEIG systems were also given. The prime mover, the induction machine, the load and the self-excitation capacitors are the four main items comprising the SEIG system. However, this thesis is focused on studying and analyzing the steady-state nonlinear behavior of the SEIG system as a nonlinear dynamic system. Poor voltage and frequency regulation are two major drawbacks of the SEIG system under variable load conditions.

# CHAPTER 5

## MODELING OF STAND- ALONE WIND-DRIVEN SEIG SYSTEM

## 5.1 MODELLING OF WIND TURBINE

The mechanical system consists of a wind turbine along with a gear box. Eq. 5.1 represents the aerodynamic power generated by wind turbine, where the aerodynamic power is expressed as a function of the specific density ( $\rho$ ) of the air in  $\text{kg/m}^3$ , the swept area of the blades ( $A$ ) in  $\text{m}^2$ , performance co-efficient of the turbine ( $C_p$ ) and the wind velocity ( $v_w$ ) in  $\text{m/s}$ [13].

$$P = 0.5\rho AC_p v_w^3 \quad (5.1)$$

For different value of wind speed a typical wind turbine speed characteristic is shown in Fig.2.4 The curve between power coefficient ( $C_p$ ) and tip speed ratio ( $\lambda$ ) at zero degree pitch angle ( $\beta$ ) is shown in Fig.2.5, which shows that  $C_p$  reaches a maximum value of 0.48 for a maximum tip speed ratio of 8.1 for any value of wind speed. Tip speed ratio of the wind turbine can be calculated using equation (2.5), where  $\omega_T$  is the rotational speed of wind turbine,  $R$  is the radius of wind turbine,  $\omega_T R$  is the linear speed at the tip of the blade.

$$\lambda = \frac{\omega_T R}{v_w} \quad (5.2)$$

The polynomial relation between  $C_p$  and  $\lambda$  at particular pitch angle for considered wind turbine [14] is represented by equation 5.3.

$$C_p(\lambda, \beta) = C_1 \left( \frac{C_2}{\lambda_i} - C_3 \beta - C_4 \right) e^{\left( \frac{-C_5}{\lambda_i} \right)} + C_6 \lambda \quad (5.3)$$

where

$$\frac{1}{\lambda_i} = \frac{1}{(\lambda + 0.08\beta)} - \frac{0.035}{(\beta^3 + 1)} \quad (5.4)$$

where  $C_1=0.5176$ ,  $C_2=116$ ,  $C_3=0.4$ ,  $C_4=5$ ,  $C_5=21$  and  $C_6=0.0068$ .

## 5.2 MODELLING OF SELF EXCITED INDUCTION GENERATOR

For the development of an induction machine model in stationary frame, the d-q arbitrary reference frame model of machine [12] is transformed into stationary reference frame. Fig 5.1 shows the schematic d-q axes diagram of SEIG. Capacitors are connected across the stator terminal to make the machine self-excited; the reference directions of currents and voltages are indicated in Fig 5.2 (a) and (b). Using d-q components of stator current ( $i_{sd}$  and  $i_{sq}$ ) and rotor current ( $i_{rd}$  and  $i_{rq}$ ) as state variables [20], the above differential equations are derived from the equivalent circuit shown in Fig. 5.2.

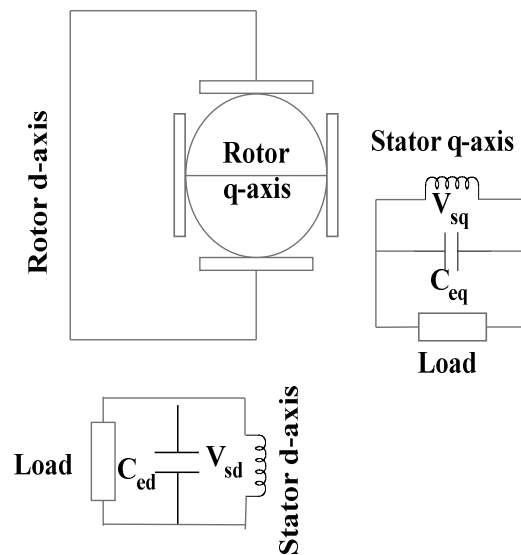


Fig. 5.1 Schematic d-q axes diagram of SEIG

In stationary reference frame the dynamic machine model can be derived by substituting  $w_e = 0$  in synchronously rotating reference frame d-q model equations. The d-q axes equivalent circuit of a (SEIG) supplying an inductive load is shown in Fig. 5.2.



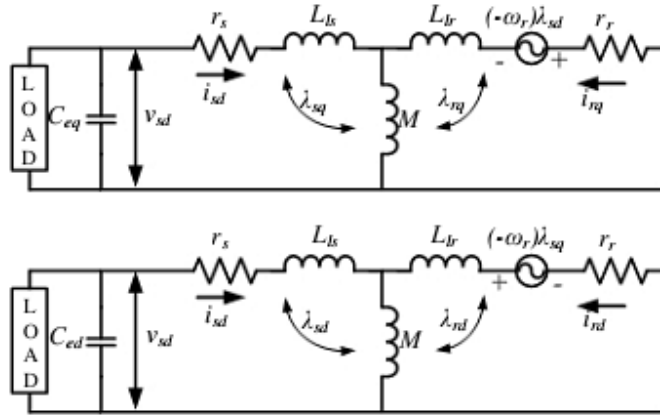


Fig.5.2 d-q model of induction machine in the stationary reference frame

(a) d-axis (b) q-axis

From above circuit by applying KVL we can get the voltage equations as follows

$$v_{qs}^s = R_s i_{qs}^s + \frac{d\lambda_{qs}^s}{dt}$$

$$v_{ds}^s = R_s i_{ds}^s + \frac{d\lambda_{ds}^s}{dt}$$

$$0 = R_r i_{qr}^s + \frac{d\lambda_{qr}^s}{dt} - \omega_r \lambda_{qr}^s$$

$$0 = R_r i_{dr}^s + \frac{d\lambda_{dr}^s}{dt} - \omega_r \lambda_{dr}^s$$

$$0 = R_r i_{qr}^s + \frac{d\lambda_{qr}^s}{dt} - \omega_r \lambda_{qr}^s$$

Where  $V_{qr} = V_{dr} = 0$

The flux linkage expressions in terms of the currents can be written from Figure

$$\lambda_{qs} = L_s i_{qs} + L_m i_{qr}$$

$$\lambda_{qr} = L_s i_{qr} + L_m i_{qs}$$

$$\lambda_{ds} = L_s i_{ds} + L_m i_{dr}$$

$$\lambda_{dr} = L_s i_{dr} + L_m i_{ds}$$

$$\frac{di_{sq}}{dt} = \frac{1}{(L_s L_r - L_m^2)} \left[ -L_s r_s i_{sq} - \omega_r L_m^2 i_{sd} + L_m r_r i_{rq} - \omega_r L_m L_r i_{rd} + L_r v_{sq} \right] \quad (5.5)$$

$$\frac{di_{sd}}{dt} = \frac{1}{(L_s L_r - L_m^2)} \left[ \omega_r L_m^2 i_{sq} - L_r r_s i_{sd} + \omega_r L_m L_r i_{rq} + L_m r_r i_{rd} + L_r v_{sd} \right] \quad (5.6)$$

$$\frac{di_{rq}}{dt} = \frac{1}{(L_s L_r - L_m^2)} \left[ L_m r_s i_{sq} + \omega_r L_m L_s i_{sd} - L_s r_r i_{rq} + \omega_r L_s L_r i_{rd} - L_m v_{sq} \right] \quad (5.7)$$

$$\frac{di_{rd}}{dt} = \frac{1}{(L_s L_r - L_m^2)} \left[ -\omega_r L_m L_s i_{sq} + L_m r_s i_{sd} - \omega_r L_s L_r i_{rq} - L_s r_r i_{rd} + L_m v_{sd} \right] \quad (5.8)$$

Where

$$L_s = L_{ls} + L_m, \quad L_r = L_{lr} + L_m$$

$$\lambda_{sq} = L_s i_{sq} + L_m i_{rq}, \quad \lambda_{sd} = L_s i_{sd} + L_m i_{rd}$$

The electromagnetic torque can be computed as a function of q and d axes stator and rotor currents and represented in equation (5.9).

$$T_e = \left( \frac{3}{2} \right) \left( \frac{P}{2} \right) L_m \left[ i_{sq} i_{rd} - i_{sd} i_{rq} \right] \quad (5.9)$$

The subscripts q and dare for quadrature and direct axes; subscripts s and r are for stator and rotor variables; l for leakage component; v and i instantaneous voltage and current;  $\lambda$  flux linkage;  $i_m$  magnetizing current;  $L_m$  magnetizing inductance; r resistance; L inductance; P number of poles;  $\omega_r$  electrical rotor speed; and  $T_e$  electromagnetic torque. The magnetization characteristic of the SEIG is nonlinear. The magnetizing inductance “ $L_m$ ” is not a constant but a function depends on the instantaneous value of magnetizing current “ $i_m$ ” given by  $L_m=f(i_m)$ .

During simulation, in each step, the magnetizing inductance “ $L_m$ ” is updated as a function of the magnetizing current “ $i_m$ ”. The magnetizing current is represented by equation (5.10).

$$i_m = \sqrt{(i_{sd} + i_{rd})^2 + (i_{sq} + i_{rq})^2} \quad (5.10)$$

The magnetizing inductance “ $L_m$ ” is calculated from the magnetizing characteristics fourth order polynomial for the test machine “ $i_m$ ”. The 4<sup>th</sup> order polynomial is arrived at, by applying curve fit technique to the relationship between “ $L_m$ ” and “ $i_m$ ”, obtained by performing synchronous speed test on the test induction machine. Torque balance equation is represented by equation (5.11).

$$T_{shaft} = T_e + J \left( \frac{2}{P} \right) \frac{dw_r}{dt} \quad (5.11)$$

The torque balance equation given in (5.11) may be expressed in speed derivative form as [9]

$$\frac{dw_r}{dt} = \left( \frac{P}{2J} \right) (T_e - T_{shaft}) \quad (5.12)$$

### 5.3 MODELLING OF EXCITATION CAPACITOR

The excitation system introduces the following state equations 5.13 and 5.14 using d-q components of stator voltage ( $v_{sd}$  &  $v_{sq}$ ) as state variables, from the circuit shown in Fig 3 (b).

$$i_{dc} = i_{ld} + i_{cd}$$

$$i_{qc} = i_{lq} + i_{cq}$$

$$\frac{dv_{ld}}{dt} = \left( \frac{i_{dc}}{C} - \frac{i_{ld}}{C} \right) \quad (5.13)$$

$$\frac{dv_{lq}}{dt} = \left( \frac{i_{qc}}{C} - \frac{i_{lq}}{C} \right) \quad (5.14)$$

## 5.4 MODELLING OF LOAD IMPEDANCE

An induction generator is self-excited by providing the magnetizing reactive power by a capacitor bank as shown in Fig 1 and the d and q axes current equations for the balanced resistive load can be given by equations 15-16.

$$i_{Rq} = \frac{v_{sq}}{R_L}$$

$$i_{Rd} = \frac{v_{sd}}{R_L}$$

And for the load considered is R-L load ( $R_L=50 \Omega$  and  $L_L= 50\text{mH}$ ). The load equations of the induction generator are represented in the same reference frame are given below.

$$v_{ld} = Ri_{ld} + \frac{di_{ld}}{dt}L$$

$$i_{ld} = \int \left[ \left( \frac{1}{L} \right) v_{ld} - \left( \frac{R}{L} \right) i_{ld} \right] \quad (5.15)$$

$$v_{lq} = Ri_{lq} + \frac{di_{lq}}{dt}L$$

$$i_{lq} = \int \left[ \left( \frac{1}{L} \right) v_{lq} - \left( \frac{R}{L} \right) i_{lq} \right] \quad (5.16)$$

If the load is capacitive in nature, then the capacitor value will be added to the excitation capacitor value.

A classical matrix formulation using d-q axes model is used to represent the dynamics of conventional induction machine operating as a generator [16, 17, 18, and 19]. Using this matrix representation, we can obtain the instantaneous voltages and currents during the self-excitation process, as well as during load variations.

$$\begin{bmatrix} \frac{di_{ds}}{dt} \\ \frac{di_{qs}}{dt} \\ \frac{di_{dr}}{dt} \\ \frac{di_{qr}}{dt} \\ \frac{dv_{ld}}{dt} \\ \frac{dv_{lq}}{dt} \\ \frac{di_{ld}}{dt} \\ \frac{di_{lq}}{dt} \end{bmatrix} = \begin{bmatrix} L_s R_s & -w_r L_m^2 & L_m R_r & w_r L_m L_r & L_r & 0 & 0 & 0 \\ w_r L_m^2 & L_r R_s & w_r L_m L_r & -L_m R_r & 0 & L_r & 0 & 0 \\ -L_m R_s & w_r L_m L_s & L_s R_r & w_r L_s L_r & -L_m & 0 & 0 & 0 \\ -w_r L_m L_s & -L_m R_s & -w_r L_s L_r & L_s R_r & 0 & -L_m & 0 & 0 \\ \frac{1}{CK} & 0 & 0 & 0 & 0 & 0 & -\frac{1}{CK} & 0 \\ 0 & \frac{1}{CK} & 0 & 0 & 0 & 0 & 0 & -\frac{1}{CK} \\ 0 & 0 & 0 & 0 & \frac{1}{LK} & 0 & \frac{-R}{LK} & 0 \\ 0 & 0 & 0 & 0 & 0 & \frac{1}{LK} & 0 & \frac{-R}{LK} \end{bmatrix} \begin{bmatrix} i_{ds} \\ i_{qs} \\ i_{dr} \\ i_{qr} \\ v_{ld} \\ v_{lq} \\ i_{ld} \\ i_{lq} \end{bmatrix} + \begin{bmatrix} -L_r & 0 & L_m & 0 \\ 0 & -L_r & 0 & L_m \\ L_m & 0 & -L_s & 0 \\ 0 & L_m & 0 & -L_s \\ 0 & 0 & 0 & 0 \\ 0 & 0 & 0 & 0 \\ 0 & 0 & 0 & 0 \\ 0 & 0 & 0 & 0 \end{bmatrix} \begin{bmatrix} v_{ds} \\ v_{qs} \\ v_{dr} \\ v_{qr} \\ 0 \\ 0 \\ 0 \\ 0 \end{bmatrix}$$

Where  $i_{ds}$ ,  $i_{dr}$ ,  $i_{qs}$ ,  $i_{qr}$  are respectively the stator and rotor currents in direct and quadrature axis and  $v_{ds}$  and  $v_{qs}$  are the initial direct axis and quadrature axis applied voltage and

$$K = \frac{1}{(L_m^2 - L_s L_r)}.$$

Combining the above expressions, the electrical transient model in terms of voltages and currents can be given in matrix form as

$$\begin{bmatrix} v_{ds} \\ v_{qs} \\ v_{dr} \\ v_{qr} \end{bmatrix} = \begin{bmatrix} R_s + \frac{dL_s}{dt} + \frac{\left(R + \frac{dL}{dt}\right)}{\frac{d^2(LR)}{dt} + RC + 1} & 0 & \frac{dLm}{dt} & 0 \\ 0 & R_s + \frac{dL_s}{dt} + \frac{\left(R + \frac{dL}{dt}\right)}{\frac{d^2(LR)}{dt} + RC + 1} & 0 & \frac{dLm}{dt} \\ \frac{dLm}{dt} & w_r L_m & \frac{dL_r}{dt} & w_r L_r \\ -w_r L_m & \frac{dLm}{dt} & -w_r L_r & \frac{dL_r}{dt} \end{bmatrix}$$

For singly fed machine, such as a cage motor in stationary frame,  $v_{qr} = v_{dr} = 0$  and  $w_e = 0$  in the above matrix.

## 5.5 DEVELOPMENT OF WIND DRIVEN SEIG DYNAMIC MODEL IN MATLAB/SIMULINK

The wind turbine acts as prime-mover for the induction machine and both are coupled through a gear box as shown in shown in Fig. 5.3 and dynamic model of Wind Driven SEIG is implemented in Simulink environment by taking equations and the flow chart in Fig.5.3. Initiation of self-excitation is based on residual magnetism in the rotor circuit and voltage builds up with the support of reactive current supplied by the capacitor bank. Load is connected to the Wind driven SEIG after the voltage is developed to a steady state value.

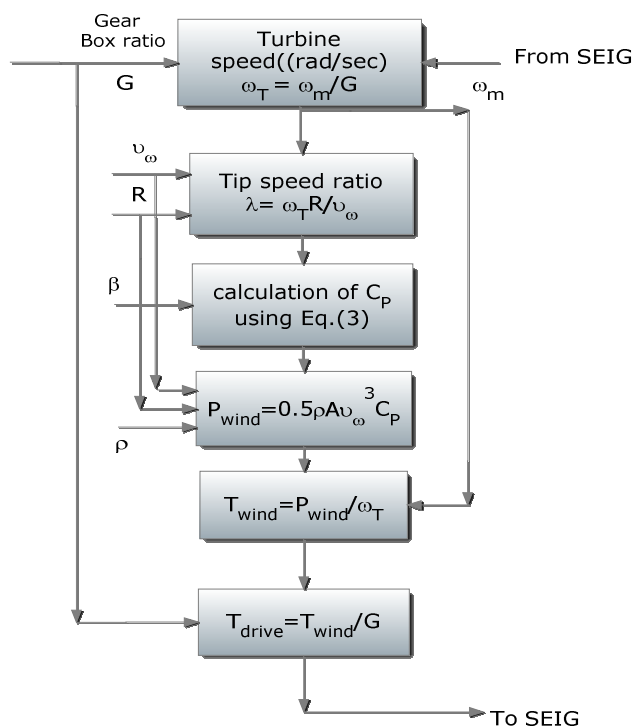


Fig 5.3. Flow chart for dynamics of Wind Turbine model

Simulation of the dynamic model of wind driven SEIG has been carried out with the view to compute the instantaneous value of currents and voltages of induction machine, the excitation system and the load. The developed dynamic model is simulated by using the numerical integration technique Runge-kutta fourth order method. For getting an accurate result, step length should be as small as possible but on the other hand it will take more time. In this case  $50\mu s$  is considered as a step time. In case of the SEIG the variation of magnetization inductance is the main factor in the dynamics of voltage build up and stabilization. From the synchronous speed test variation of magnetizing inductance " $L_m$ " is obtained with respect to " $i_m$ ". Before simulation is run, it is necessary to provide initial values of the input states of the q-d model of the induction generator. The initial values of the currents " $i_{sd}$ ", " $i_{sq}$ ", " $i_{rd}$ " and " $i_{rq}$ " are assumed to be zero. For the purpose of self-excitation, the residual magnetism of the machine is taken as initial values of " $v_{sd}$ " and " $v_{sq}$ ". The simulation results of wind driven SEIG in isolated mode are discussed in the next section.

## 5.6 SUMMARY

The chapter presents the mathematical modeling equations for different parameters of wind turbine, self-excited induction generator, excitation capacitor and load impedance. Using all these d-q equations of machine a classical matrix is formulated which is used to represent the dynamics of conventional induction machine operating as a generator. By using these equations in Matlab/Simulink a wind driven self-excited induction generator can be implemented. This chapter also explains the flow chart for dynamics of Wind Turbine model.

# CHAPTER 6

## RESULTS & DISCUSSION



## 6.1 SIMULATION RESULTS

Specifications of wind turbines and induction Machines taken for the simulation is given in tables. The magnetization curve for the above machines are expressed in terms of  $L_m$  (H) Vs  $i_m$ (A) is given in table 3 and table 6.

**Table-1** (Wind turbine coupled with 22kW induction machine)

Rated Power (kW)	25
Diameter ( m)	12.8
No. of Blades	3
Cut-in wind Speed	3 m/s
Cut-out wind speed	25 m/s

**Table-2**(Induction machine 22 kW,3-phase,4 Pole star connected,415 volt,50 hz)

$R_s$ ( $\Omega$ )	$R_r$ ( $\Omega$ )	$X_{ls}$ ( $\Omega$ )	$X_{lr}$ ( $\Omega$ )	$L_m$ (H)	$J$ ( $\text{kg m}^2$ )
0.2511	0.2489	0.439	0.439	0.0591	0.305

**Table-3**( $L_m$  vs  $i_m$ )

$i_m$ (A)	$L_m$ (H)
$\leq 8$	0.075
8- 13	$0.075 - .003(i_m-8)$
13- 23	$0.06 - .002(i_m-13)$
$\geq 23$	0.041

**Table-4**(Wind turbine coupled with 7.5 kW induction machine)

Rated Power (kW)	10
Diameter ( m)	8
No. of Blades	3
Rated wind Speed	10 m/s

**Table-5** (Induction machine 7.5 kW,3-phase,4 pole star-delta connected,415 volt,50 hz)

$R_s$ ( $\Omega$ )	$R_r$ ( $\Omega$ )	$X_{ls}$ ( $\Omega$ )	$X_{lr}$ ( $\Omega$ )	$L_m$ (H)	$J$ ( $\text{kg m}^2$ )
1	0.77	1.5	1.5	0.134	0.1384

**Table-6**( $L_m$  vs  $i_m$ )

$I_m$ (A)	$L_m$ (H)
$\leq 3.16$	0.134
3.16 - 12.72	$9e-5I_m^2 - 0.0087I_m + 0.1643$
$\geq 12.72$	0.068

The transient behavior of 22 kW, 7.5 kW SEIG coupled with wind turbine, specifications are given in the above tables having balanced delta-connected excitation capacitor across the terminal of SEIG has been studied. The transient behavior of the wind driven SEIG under the following condition has been observed.

1. Self-excitation process
2. Insertion of load
3. Loss of excitation due to heavy-load
4. Insertion of excitation capacitor
5. Change in wind velocity

### 6.1.1 Self-excitation Process

The fixed excitation capacitance is selected as 152  $\mu\text{F}$ , for the 22 kW induction machine data is given in table 1 taken from [6]. The SEIG driven by wind turbine with wind velocity of 12.6 m/s at no load and the simulation results are shown in Fig. 6.1-6.5. It is observed that the residual magnetism taken in terms of  $V_{sd}$  and  $V_{sq}$  as 1 volt for the simulation induces a voltage across the self-exciting capacitor and produces a capacitive current or a lagging magnetizing current in the stator winding and result a higher voltage. This procedure goes on until the saturation of the

magnetic field occurs as observed in the simulation results shown in Fig. 6.2 and 6.3. It is also observed that for SEIG rotor speed of 1725 r.p.m shown in Fig. 6.1, the voltage and current waveform of SEIG reach the steady state condition within 7.38 sec following the voltage build up process. The steady state magnitude of the peak SEIG terminal voltage is 337 volts(rms236 ) and stator current is 18.44 amps at no load shown in Fig. 6.4 and Fig. 6.5

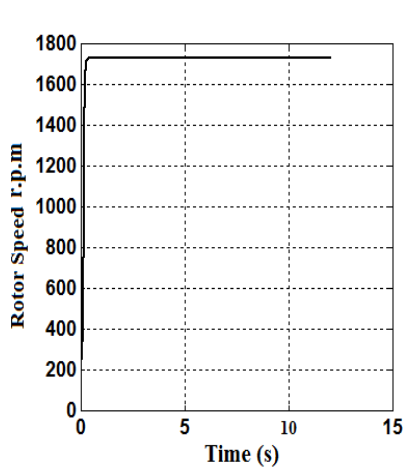


Fig.6.1 SEIG Rotor speed

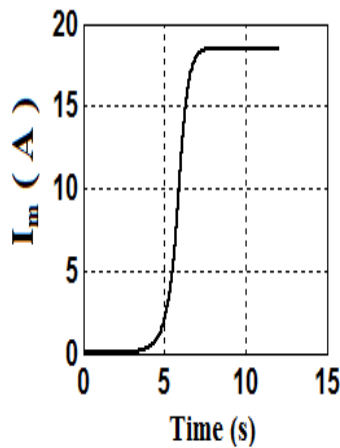


Fig. 6.2 Magnetizing current

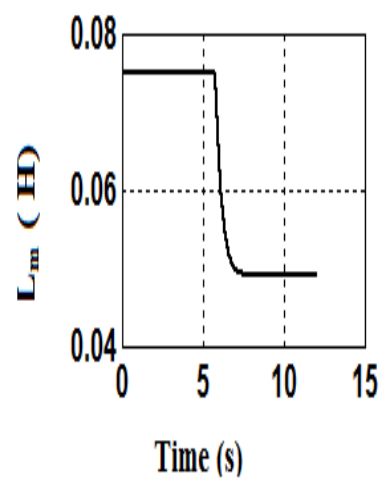


Fig.6.3Magnetizing Inductance

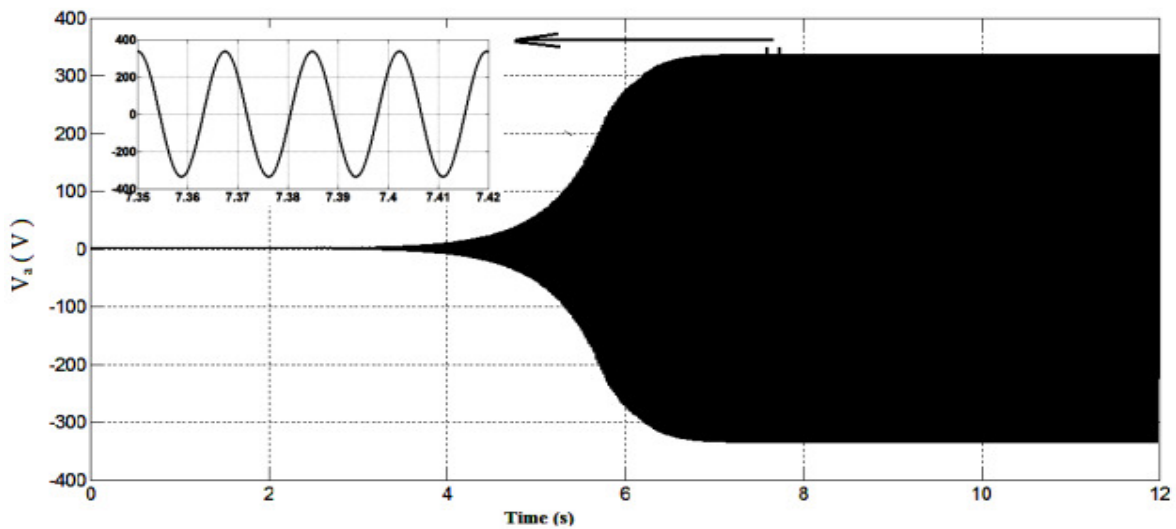


Fig.6.4 Stator terminal Voltage

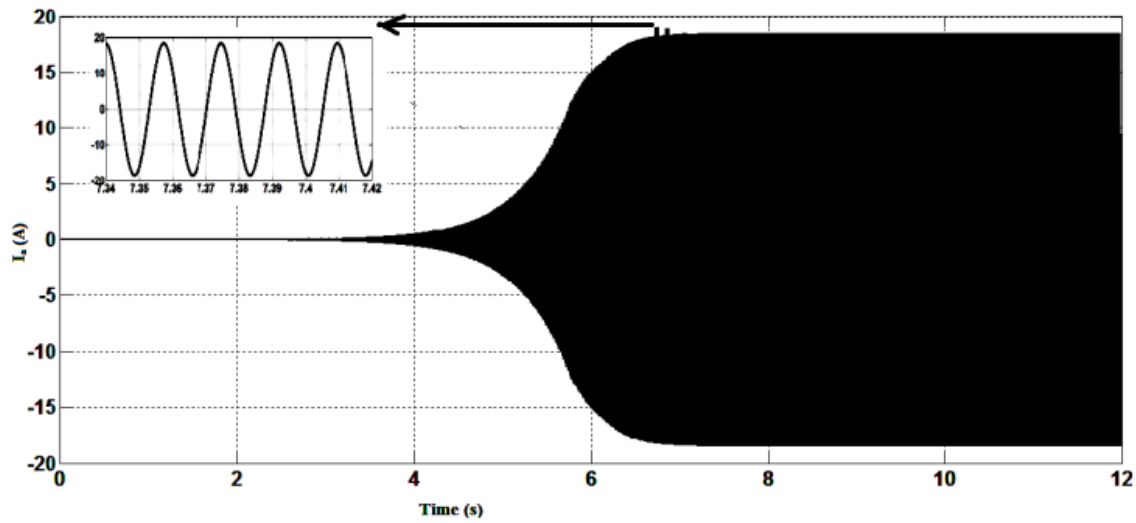


Fig.6.5 Stator current wave form

### 6.1.2 Insertion of Load

Fig. 6.6-6.10 are the simulation results of 7.5 kW induction machine at constant wind speed of 11m/s for R-L load having p.f 0.8 applied at  $t=5$  seconds. It is observed that steady state peak voltage is 332 volt at no load, reduces to 193 volt and speed reduces from 1720 r.p.m to 1705 r.p.m shown in Fig.6.6 and 6.8. When the SEIG is operating at no-load, the load current is zero, the load current reaches a steady-state value of 2.96 amperes (peak amplitude) shown in Fig.6.11. Loading decreases the magnetizing current  $I_m$  shown in Fig.6.10 which results in the reduced flux. Reduced flux implies reduced voltage.

### 6.1.3 Loss of Excitation due to heavy-load

The SEIG which is initially operated under steady state condition having peak value of voltage 332 volts and R-L load is applied at  $t=5$  seconds having p.f 0.8, voltage is reduced and reached a steady state voltage of 193 volt. At  $t=8$  seconds an extra load is applied, the SEIG line voltage collapse is a monotonous decay of the voltage to zero shown in Fig.6.12. Once the voltage collapse occurs, the re-excitation of the generator becomes difficult. Thus it shows the poor overloading capability of the SEIG. Therefore the load connected to the generator should never

exceed beyond the maximum load the generator can deliver under steady state condition. But it may be mentioned here that the momentary excess stator current can operate protective relays to isolate the overload condition at the generator terminals to prevent voltage collapse.

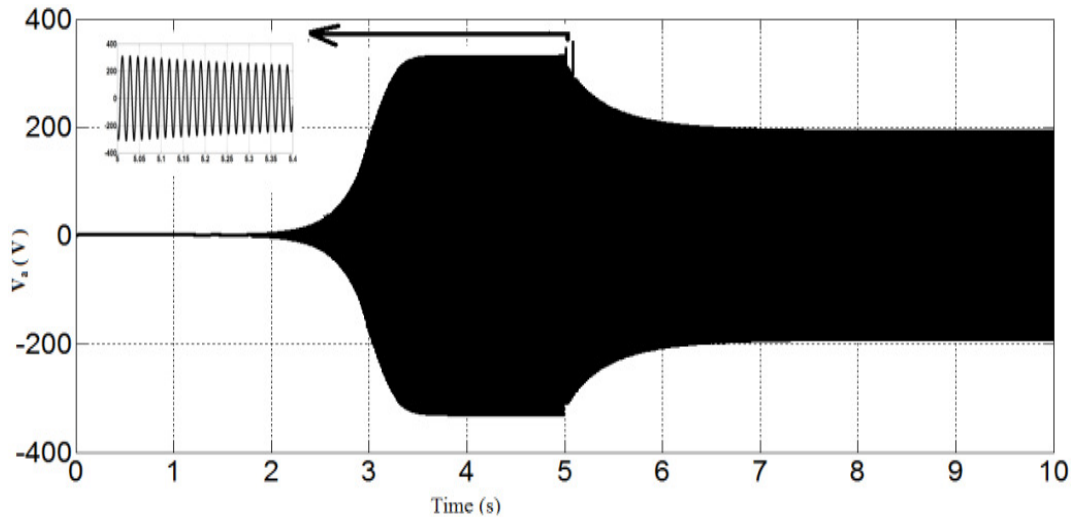


Fig.6.6 SEIG Stator terminal Voltage

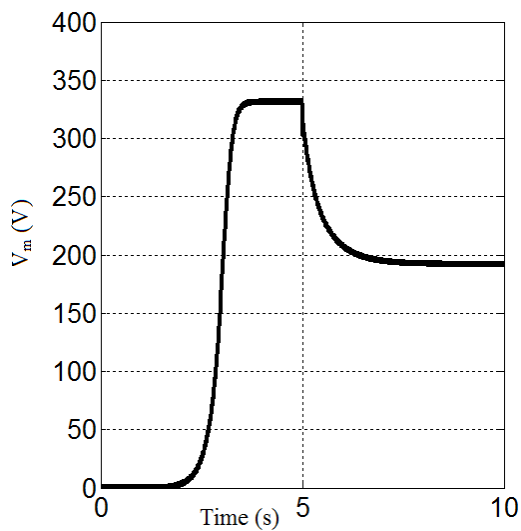


Fig.6.7 Peak SEIG terminal voltage/phase

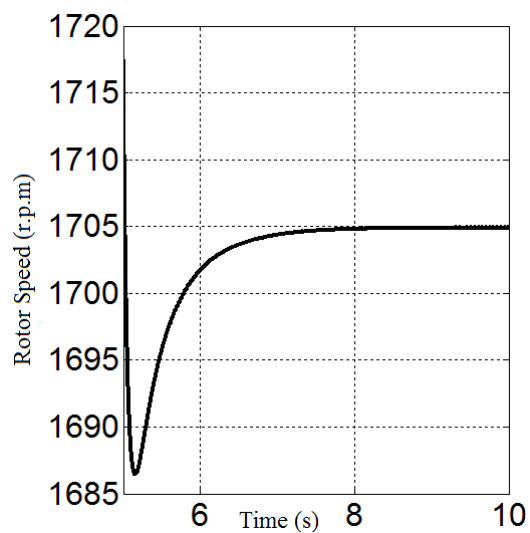


Fig.6.8 SEIG rotor speed variation with load

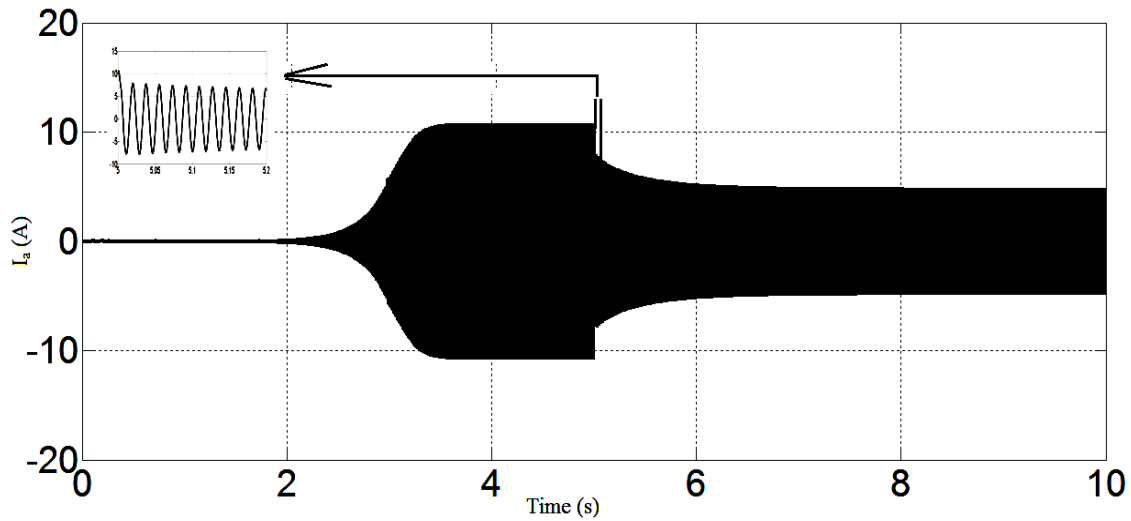


Fig. 6.9 SEIG stator current waveform

### 6.1.4 Insertion of Excitation Capacitor

The SEIG is initially operated under steady state condition with three-phase balanced delta-connected capacitor bank of  $90 \mu\text{F}/\text{phase}$  connected across its stator terminal while resistive load of  $80 \Omega$  is connected at  $t=5$  seconds, the steady state voltage is reduced from 332 volts to 305 volts. The increase in load current should be compensated either by increasing the energy input (drive torque) thereby increasing the rotor speed or by an increase in the reactive power to the generator. At  $t=7$  excitation capacitor of  $10 \mu\text{F}/\text{phase}$  is added to the existing value. The corresponding simulation results are shown in Fig.6.13–6.17. It is observed from Fig. 6.13 that the peak magnitude of stator voltage increases to 316 volts with the addition of excitation capacitor value. Fig.6.16 and 6.17 represents the real power variation and reactive power variation due to addition of load at  $t=5$  sec and insertion of excitation capacitor at  $t=7$  sec.

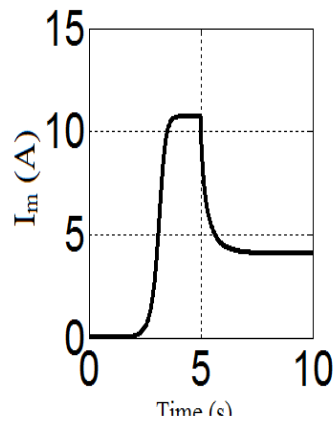


Fig.6.10 Variation of  $I_m$  with load

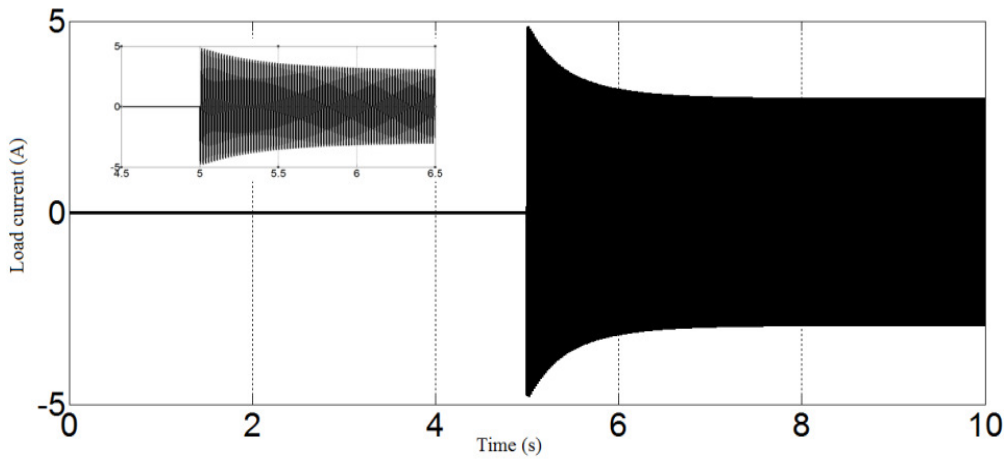


Fig.6.11 Load current variation with load

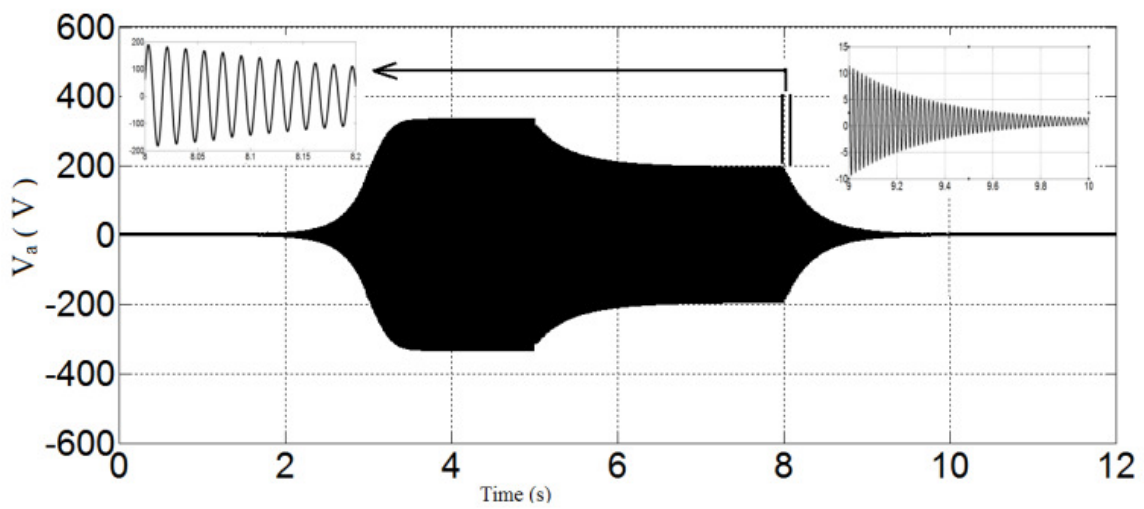


Fig.6.12 Loss of excitation

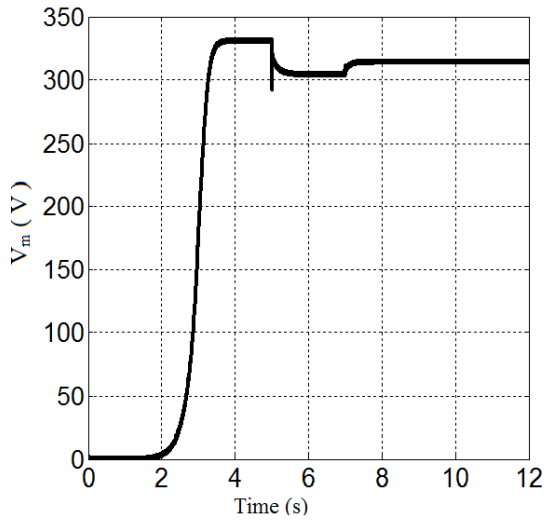


Fig.6.13 Peak SEIG terminal voltage/phase

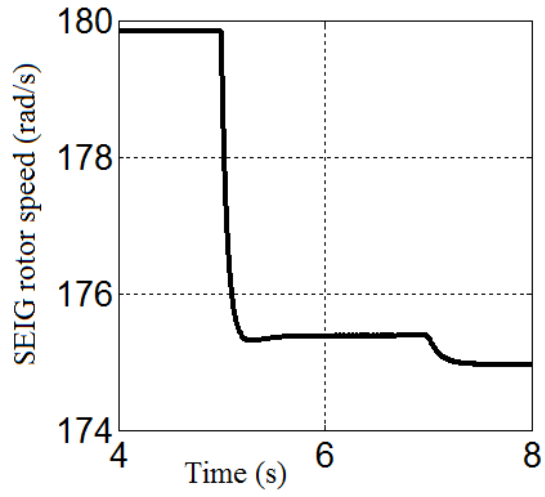


Fig.6.14 Rotor speed variation with load and addition of capacitor

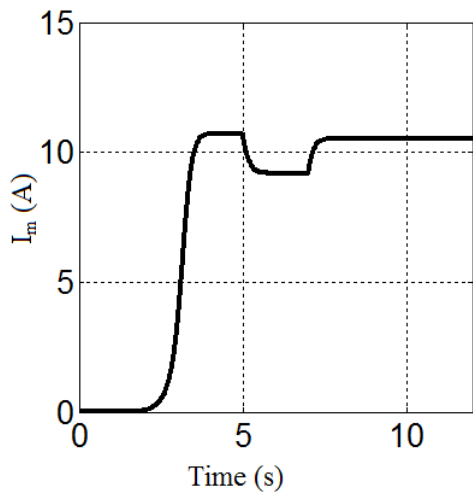


Fig.6.15  $I_m$  Variation

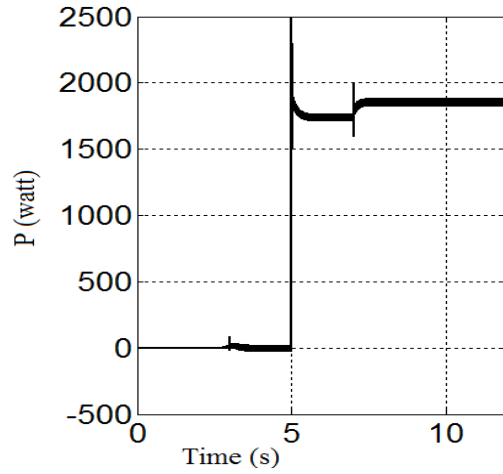


Fig.6.16 Real power variation



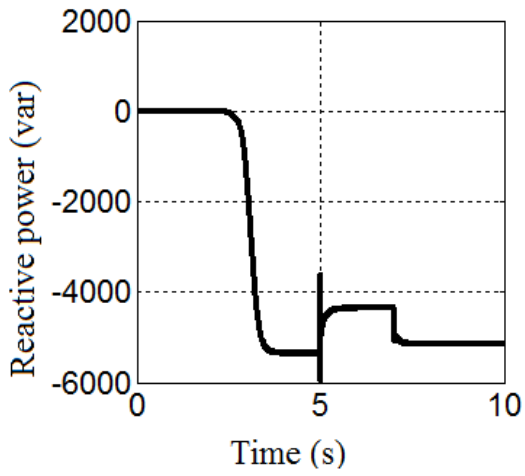


Fig.6.17 Reactive power variation

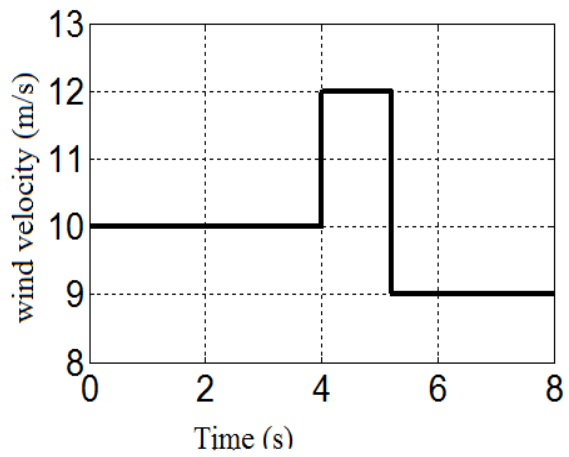


Fig.6.18 Step change in wind velocity

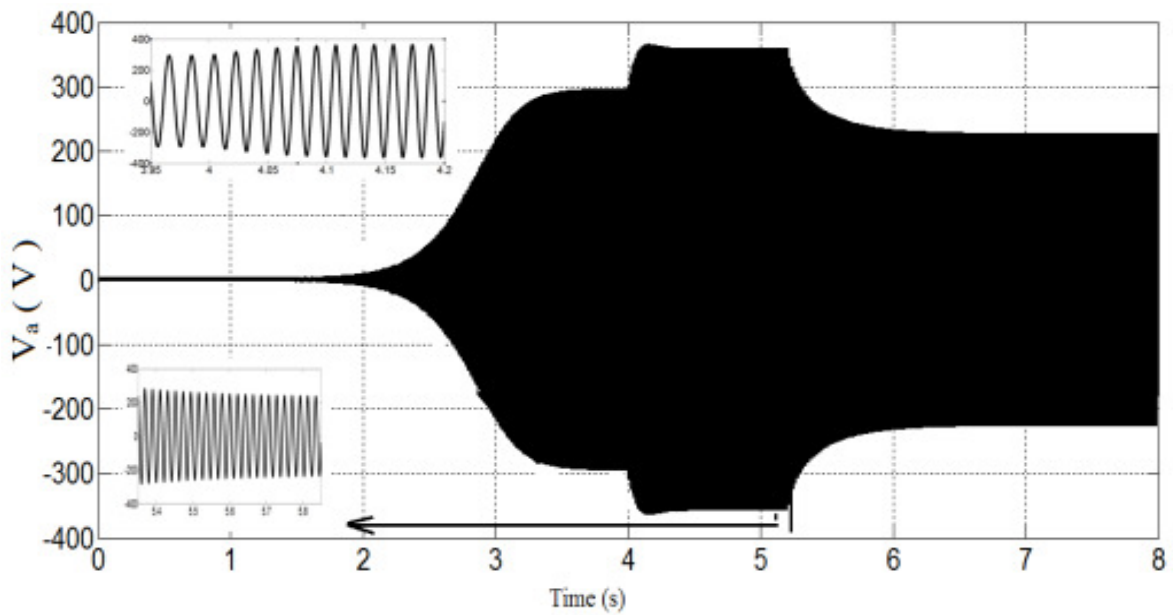


Fig.6.19 Stator voltage variation with step change in wind velocity

### 6.1.5 Step change in wind velocity

Simulation results with step change in wind velocity are shown in Fig. 6.18-6.21, as the wind velocity increases from 10 m/s to 12 m/s at  $t = 4$  seconds, the mechanical input from the wind

turbine increases and this result in the increased rotor speed causing an increase in the stator terminal voltage. When wind velocity decreases from 12 m/s to 9 m/s at  $t = 5$  seconds, rotor speed decreases and hence decreases the stator terminal voltage of SEIG.

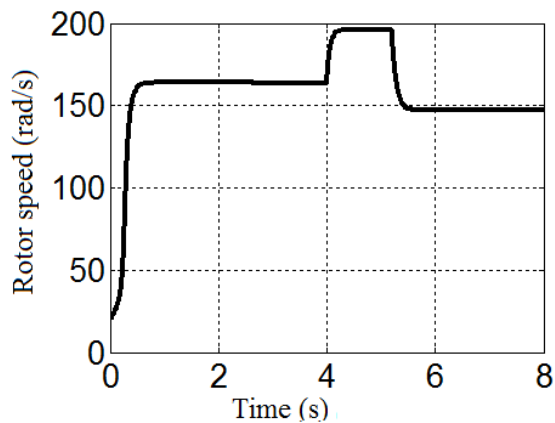


Fig.6.20 Rotor speed variation with Step change in wind velocity

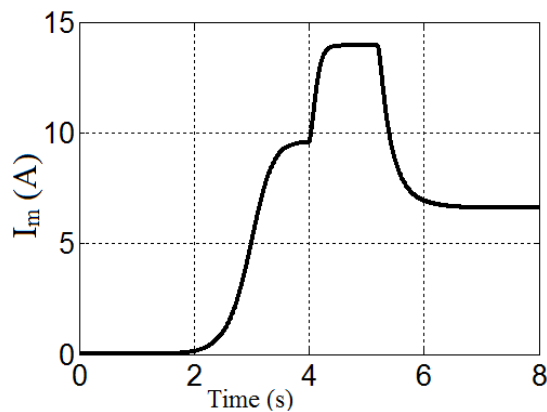


Fig.6.21  $I_m$  Variation

## 6.2 EXPERIMENTAL RESULTS

Conducted the open loop experiment with the available 5 hp induction machine in the machines laboratory. The experimental set up is as shown in below figure. Lamp load is also connected to the machine. Initially capacitors are charged for few minutes by giving three phase supply to provide reactive power to the induction machine when it is operating as induction generator. Now by giving DC supply to the DC shunt motor which acts like prime mover for the induction machine. By adjusting the rheostats connected in armature and field circuit of DC motor the induction machine is made to run above synchronous speed Now the machine acts as induction generator by taking reactive power from the capacitors connected across stator of the machine. The generated waveforms are observed in the CRO.



Fig.6.22 Experimental setup

We can observe the buildup of voltage from zero to 415v and after some time due to saturation voltage getting settled at 415v.

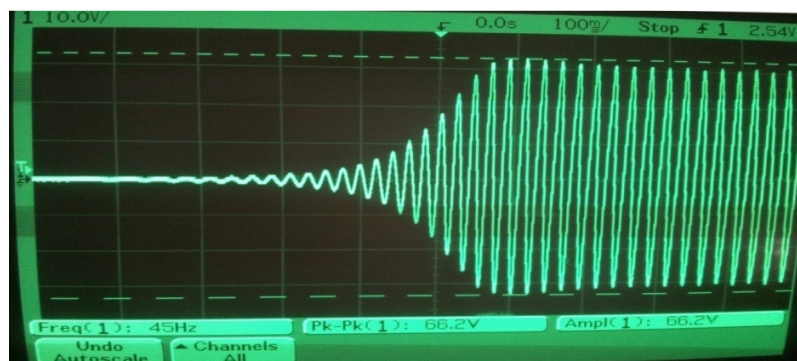


Fig.6.23 Build up of Line Voltage

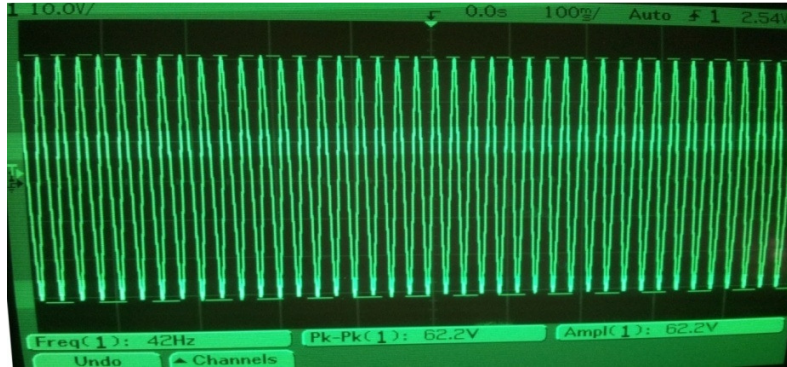


Fig.6.24 Settled voltage

**By applying load**

Hera we can also observed the decrease in generated voltage when load is applied on the induction machine.

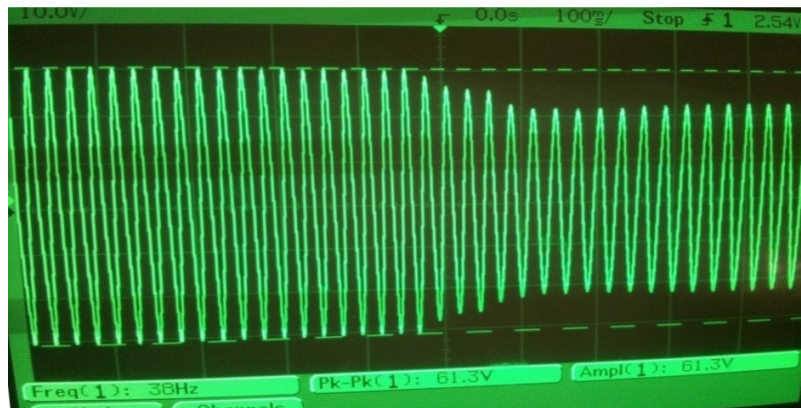


Fig.6.25 Decrease in voltage by releasing Load

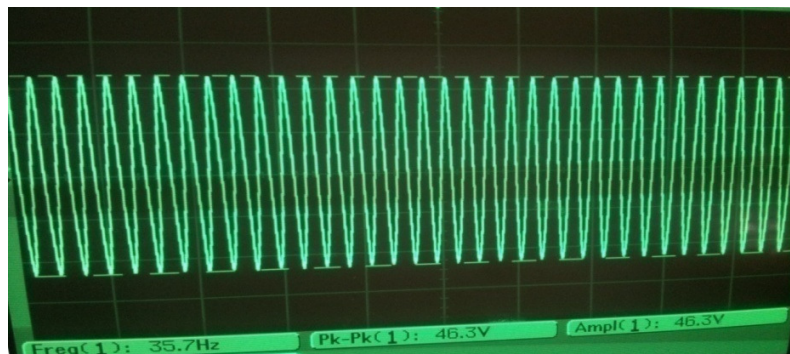


Fig.6.26 Reduced voltage after releasing Load



### By releasing the load

Here we can observe the increase in voltage when the load on the induction machine is released.

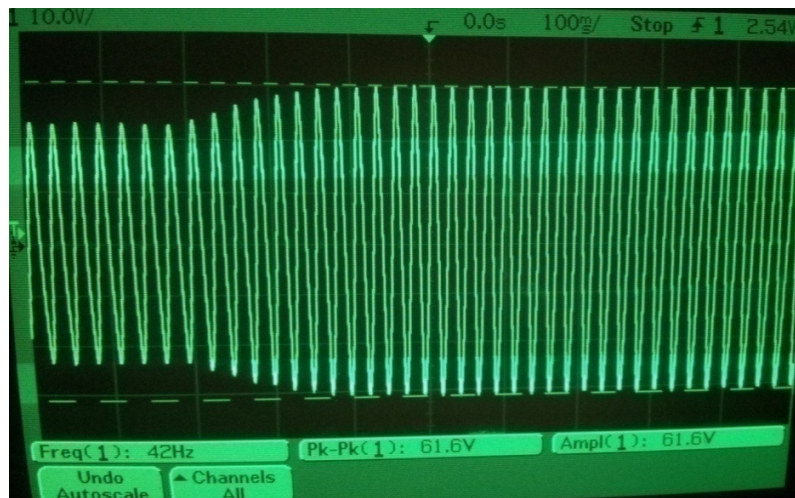


Fig.6.27 Increase in voltage by releasing Load

# CHAPTER 7

## CONCLUSION & SCOPE OF FUTURE WORK

## **7.1 CONCLUSION**

In this paper, d-q model of self-excited induction generator driven by variable speed prime movers and in particular by wind turbines in stationary reference frame developed. Voltage build up process of a SEIG is presented both for no load and loaded condition using MATLAB/Simulink and experimental result reveals that magnitude of voltage decreases with load. And it is concluded that voltage developed depends on three factors: (i) speed of the rotor, (ii) capacitor value connected for excitation and (iii) load connected across the stator terminal. Experimentally verified the open loop control on self-excited induction generator in the laboratory. It is anticipated that the model presented in this paper would be broadly applicable in any system where the induction machine is used as a generator.

## **7.2 SCOPE OF FUTURE WORK**

As concluded above the voltage developed in a stand-alone self-excited induction generator depends upon excitation value of capacitor, load and speed of the rotor. So voltage varies and to maintain it constant a controller is required. For stand-alone system controller should be such that it is simple and has faster response. A laboratory-scale stand-alone SEIG system with simple and reliable controller can be developed by taking balanced, un-balanced, non-linear and dynamic load conditions.

## REFERENCES

- [1] G.M. Joselin Herbert , S. Iniyan , E. Sreevalsan , S. Rajapandian “ A review of wind energy technologies” Renewable and Sustainable Energy Reviews 11 (2007), pp. 1117–1145
- [2] G.K. Singh “ Self-excited induction generator research—a survey” Electric Power Systems Research 69 (2004), pp. 107–114
- [3] S. Nikolova , A. Causevski , A. Al-Salaymeh “Optimal operation of conventional power plants in power system with integrated renewable energy sources” Energy Conversion and Management 65(2013), pp. 697–703
- [4] G. D. Rai, “Non - Conventional Energy Sources”, Khanna publishers.
- [5] J.G. Sloopweg and W.L. Kling, “Is the Answer Blo”, IEEE Power & Energy magazine november/December 2003, pp3 26-33
- [6] Bimal K. Bose “Modern Power Electronics and AC Drives” PHI Learning private Limited.
- [7] Mahmoud M. Neam, Fayez F. M. El-Sousy, Mohamed A. Ghazy and Maged A. Abo-Adma, “ The Dynamic Performance of an Isolated Self Excited Induction Generator Driven by a Variable-Speed Wind Turbine” IEEE Trans.2007, pp. 536-543
- [8] R. C. Bansal, T. S. Bhatti, and D. P. Kothari, “A bibliographical survey on induction generators for application of nonconventional energy systems,” IEEE Trans. Energy Convers., vol. 18, no. 3, pp. 433-439, September 2003.
- [9] M. G. Simões and F. A. Farret, Alternative Energy Systems: Design and Analysis with Induction Generators, Bosa Roca: Taylor & Francis, December 2007.
- [10] R. C. Bansal, “Three-Phase Self-Excited Induction Generators: An Overview,” IEEE Transactions on Energy Conversion, vol. 20, no. 2, pp.292-299, June 2005.
- [11] E. Levy and Y. W. Liao, “An Experimental Investigation of Self-excitation in Capacitor Excited Induction Generators,” Electric Power System Research, vol. 53, no. 1, pp. 59-65, January 2000.
- [12] E. Suarez and G. Bortolotto, “Voltage-frequency Control of a Self-excited Induction Generator,” IEEE Transactions on Energy Conversion, vol. 14, no. 3, pp. 394-401, September 1999.



- [13] H. Geng, D. Xu and B. Wuare, "Direct voltage control for a stand-alone wind-driven self-excited induction generator with improved power quality," *IEEE Trans. on Power Elect.*, vol. 26, no. 8, August 2011, pp. 632-641.
- [14] A. Karthikeyan, C. Nagamani, G. Saravana, A. Sreenivasulu, "Hybrid, open-loop excitation system for a wind turbine driven stand-alone induction generator" *IET Renew. on Power Gener.*, vol. 5, no. 2, 2011, pp. 184-193.
- [15] T. Burton, D. Sharpe, N. Jenkins, and E. Bossanyi, *Wind Energy Handbook*, John Wiley & Sons Ltd., Chichester, England, 2001.
- [16] B. Singh and L. B. Shilpakar, "Analysis of a novel solid state voltage regulator for a self-excited induction generator", *IEE Proc-GenerTransmDistrib*, vol. 145, no. 6, November 1998, pp. 647-655.
- [17] Jayalakshmi N.S. and D.N. Gaonkar, "Dynamic Modeling and Analysis of an Isolated self-excited induction generator driven by wind turbine", *IEEE Trans.* 2012, pp. 1-5
- [18] Avinash Kishore, G. Satish Kumar, "A Generalized State-Space Modeling of Three Phase Self-Excited Induction Generator For Dynamic Characteristics and Analysis", *IEEE Trans. at. ICIEA 2006*
- [19] Birendra Kumar Debta, Kanungo Barada Mohanty "Analysis, Voltage Control and Experiments on a Self-Excited Induction Generator".
- [20] K. Trinadha, A. Kumar, K. S. Sandhu, "Study of Wind Turbine based SEIG under Balanced/Unbalanced Loads and Excitation" *International Journal of Electrical and Computer Engineering (IJECE)* Vol.2, No.3, June 2012, pp. 353-370
- [21] A. Kishore, R. C. Prasad, and B. M. Karan, "MATLAB SIMULINK Based DQ Modeling and Dynamic Characteristics of Three Phase Self Excited Induction Generator", *Progress In Electromagnetics Research Symposium 2006*, Cambridge, USA, March, pp. 26-29
- [22] D. Seyoum, C. Grantham, and M.F. Rahman, "The dynamic characteristics of an isolated generator driven by a wind turbine," *IEEE Trans. on Ind. Appl.*, vol. 39, no.4, pp. 936-944. July/ August 2003.